Journal of Human Evolution 97 (2016) 123–144

Contents lists available at ScienceDirect

Journal of Human Evolution

journal homepage: www.elsevier.com/locate/jhevol

Internal carotid arterial canal size and scaling in Euarchonta: Re-assessing implications for arterial patency and phylogenetic relationships in early fossil primates

Doug M. Boyer [a, b, *], E. Christopher Kirk [d, e], Mary T. Silcox [h], Gregg F. Gunnell [a, b, c], Christopher C. Gilbert [c, f], Gabriel S. Yapuncich [a], Kari L. Allen [g], Emma Welch [a], Jonathan I. Bloch [i], Lauren A. Gonzales [a], Richard F. Kay [a], Erik R. Seiffert [b, j]

[a] Department of Evolutionary Anthropology, Duke University, Durham, NC 27708, USA
[b] Division of Fossil Primates, Duke Lemur Center, Durham, NC 27705, USA
[c] New York Consortium in Evolutionary Primatology (NYCEP), American Museum of Natural History, New York, NY 10024, USA
[d] Department of Anthropology, University of Texas, Austin, Austin, TX, USA
[e] Jackson School Museum of Earth History, University of Texas, Austin, Austin, TX, USA
[f] Department of Anthropology, Hunter College of the City University of New York, 695 Park Avenue, New York, NY 10065, USA
[g] Department of Anatomy and Neurobiology, Washington University School of Medicine in St. Louis, St. Louis, MO, USA
[h] Department of Anthropology, University of Toronto Scarborough, Scarborough, Ontario M1C 1A4, Canada
[i] Department of Vertebrate Paleontology, University of Florida, Florida Museum of Natural History, Gainesville, FL 32611, USA
[j] Department of Cell and Neurobiology, Keck School of Medicine, University of Southern California, Los Angeles, CA 90033, USA

ARTICLE INFO

Article history:
Received 4 March 2016
Accepted 4 June 2016

Keywords:
Brain
Petrosal
Stapedial artery
Internal carotid artery
Allometry
Adapiforms
Omomyiforms

ABSTRACT

Primate species typically differ from other mammals in having bony canals that enclose the branches of the internal carotid artery (ICA) as they pass through the middle ear. The presence and relative size of these canals varies among major primate clades. As a result, differences in the anatomy of the canals for the promontorial and stapedial branches of the ICA have been cited as evidence of either haplorhine or strepsirrhine affinities among otherwise enigmatic early fossil euprimates. Here we use micro X-ray computed tomography to compile the largest quantitative dataset on ICA canal sizes. The data suggest greater variation of the ICA canals within some groups than has been previously appreciated. For example, *Lepilemur* and *Avahi* differ from most other lemuriforms in having a larger promontorial canal than stapedial canal. Furthermore, various lemurids are intraspecifically variable in relative canal size, with the promontorial canal being larger than the stapedial canal in some individuals but not others. In species where the promontorial artery supplies the brain with blood, the size of the promontorial canal is significantly correlated with endocranial volume (ECV). Among species with alternate routes of encephalic blood supply, the promontorial canal is highly reduced relative to ECV, and correlated with both ECV and cranium size. Ancestral state reconstructions incorporating data from fossils suggest that the last common ancestor of living primates had promontorial and stapedial canals that were similar to each other in size and large relative to ECV. We conclude that the plesiomorphic condition for crown primates is to have a patent promontorial artery supplying the brain and a patent stapedial artery for various non-encephalic structures. This inferred ancestral condition is exhibited by treeshrews and most early fossil euprimates, while extant primates exhibit reduction in one canal or another. The only early fossils deviating from this plesiomorphic condition are *Adapis parisiensis* with a reduced promontorial canal, and *Rooneyia* and *Mahgarita* with reduced stapedial canals.

1. Introduction

In primitive eutherian mammals, the internal carotid artery (ICA) is hypothesized to have divided into two major branches as it passed through the middle ear (MacPhee and Cartmill, 1986; Wible,

* Corresponding author.
E-mail address: doug.boyer@duke.edu (D.M. Boyer).

http://dx.doi.org/10.1016/j.jhevol.2016.06.002
0047-2484/

1986, 1987). The promontory artery, named for its course adjacent to the promontorium of the petrosal (i.e., the bulge of the cochlea into the middle ear space), supplied blood to the brain via the cerebral arterial circle (of Willis) (Saban, 1963, 1975; Bugge, 1974; MacPhee and Cartmill, 1986). The stapedial artery, named for its passage through the obturator foramen of the stapes, supplied blood to the meninges, eye, orbit, and parts of the face (Saban, 1963; Bugge, 1974; Wible, 1987). Although several branches of the stapedial artery were evidently lost early in primate evolution (e.g., ramus posterior and inferior; Bugge, 1974; Cartmill and MacPhee, 1980; MacPhee, 1981), all euarchontans (the group including primates and their close relatives: dermopterans and scandentians) that have been examined ontogenetically exhibit this plesiomorphic pattern of cranial vasculature early in fetal development (MacPhee, 1981; Wible, 1993; Wible and Martin, 1993). Extant primates vary, however, in (1) whether the ICA and its branches are maintained into adulthood and (2) the relative sizes of the branches that persist (Cartmill, 1975; MacPhee, 1981; MacPhee and Cartmill, 1986; Wible and Martin, 1993).

Differences in ICA anatomy among living primates distinguish three main groups. In extant haplorhines, the ICA and promontory artery remain patent in adults, but the territory of the fetal stapedial artery is largely annexed by branches of the external carotid artery during ontogeny. As a result, the stapedial artery is either absent (anthropoids) or variably absent and exceedingly small (adult tarsiers) (MacPhee and Cartmill, 1986). In non-cheirogaleid lemuriforms, the ICA and stapedial artery are retained, but adults are thought to either lack a promontory artery altogether, or to variably retain a small promontory artery (Bugge, 1974; Conroy and Wible, 1978; MacPhee and Cartmill, 1986), meaning that the promontorial artery cannot form a critical blood supply route for the brain in these lemuriform taxa. In lorisiforms and cheirogaleids, the entire ICA involutes during ontogeny and the territories of both the fetal promontorial and stapedial arteries are annexed by the external carotid artery (ECA) during development, with the ascending pharyngeal artery (a branch of the ECA) providing significant blood supply to the brain (Cartmill, 1975; MacPhee, 1981). As a result, lorisiforms and cheirogaleids differ from other living primates in lacking both the promontory and stapedial arteries as adults.

In primates that retain the ICA, there is a bony canal for this artery that is derived from the petrosal. Similarly, primates that retain patent promontorial and/or stapedial arteries into adulthood typically enclose portions of these arteries in bony canals derived from the petrosal. Among extant placental mammals, such enclosure of the intra-tympanic branches of the ICA in bony canals otherwise occurs in scandentians, in some members of Afrotheria (chrysochlorids and macroscelideans), Glires (stapedial artery only), and Eulipotyphla (Bugge, 1974; MacPhee, 1981; MacPhee et al., 1988; Meng et al., 2003; Mason, 2004; Wible, 2011), although these bony canals are not always petrosal or wholly petrosal in origin (Cartmill and MacPhee, 1980; MacPhee, 1981; Wible, 2011). In taxa lacking bony canals for the branches of the ICA, the petrosal often exhibits grooves that document the sizes and pathways of the promontorial and stapedial arteries (e.g., MacPhee et al., 1988).

The enclosure of the ICA and its dependencies in bony canals or grooves provides an opportunity to assess ICA anatomy in many fossil taxa using osteological criteria. For example, omomyiforms have been interpreted as “haplorhine-like” (Szalay, 1975; MacPhee and Cartmill, 1986) based on the presence of a larger promontorial canal than stapedial canal. Adapiforms have been variously interpreted as “strepsirrhine-like” (MacPhee and Cartmill, 1986; Rose et al., 1999) or “haplorhine-like” (Gingerich, 1973, 2012) due to differing perspectives on whether the promontorial canal is significantly enlarged relative to the stapedial canal (Rasmussen, 1990; Ross, 1994; Kirk et al., 2014). Yet other authors have concluded that omomyiforms and adapiforms are both “primitive” in retaining promontorial and stapedial canals that are both “large” (Saban, 1963; Bugge, 1974; Cartmill et al., 1981; Ross and Covert, 2000). Admittedly, some of the diversity in perspective seems to reflect real interspecific differences among members of these groups (MacPhee and Cartmill, 1986). For instance, *Adapis* (MacPhee and Cartmill, 1986) and early *Cantius* (Rose et al., 1999) have been described as having promontorial canals that are smaller than their stapedial canals, and partially open (not enclosed fully in bone), whereas *Notharctus* and *Smilodectes* (likely sister taxa or descendants of *Cantius*) have been described as having promontorial canals that are larger than their stapedial canals and fully enclosed in bone (Gingerich, 1973; MacPhee and Cartmill, 1986). In the enigmatic adapiform *Mahgarita stevensi*, the stapedial canal is clearly miniscule (nearly lost) compared to the promontorial canal. Researchers differ on whether this counts as a haplorhine synapomorphy (Rasmussen, 1990) or a convergent reduction of the stapedial canal in a strepsirrhine (Ross, 1994). Nonetheless, in many cases the same taxon has been interpreted in contradictory ways by different authors, revealing a problematic subjectivity in assessments of promontorial and stapedial canal size. For instance, though the promontorial canal is clearly bigger than the stapedial canal in *Notharctus*, Ross (1994), Bugge (1980), and Saban (1963) consider that both canals are still big enough to reflect the primitive condition of primates, whereas Gingerich (1973, 2012) considers *Notharctus* to show an affinity to haplorhines in its degree of stapedial reduction. As another example, *Necrolemur* has a smaller stapedial canal than promontorial canal. Acknowledging this, Cartmill et al. (1981) and Bugge (1980) consider the canals to be ‘subequal’ and conclude that the condition is probably primitive, whereas Szalay (1975) considers the smaller stapedial canal in *Necrolemur* to indicate haplorhine affinities.

Resolution of these contradictions requires more quantitative comparative data and a better understanding of intra- and interspecific variation in bony anatomy associated with the ICA among crown primates. In particular, it is necessary to consider whether there is any basis for looking at the size of the promontorial and stapedial canals *in relation to one another*, which is often how canal size has been assessed in fossils (Gingerich, 1973; Szalay, 1975; MacPhee and Cartmill, 1986; MacPhee et al., 1988; Gingerich, 2012). Furthermore, when studies conclude that omomyiforms and adapiforms are “primitive” they are interpreting them as similar to scandentians in having promontorial and stapedial canals that are “large” (Saban, 1963; Bugge, 1980; MacPhee et al., 1988; Ross, 1994; Ross and Covert, 2000). The question of whether both canals are large or small has to be considered with respect to some other aspect of an animal's anatomy, but previous work has not been explicit or consistent in stating the other aspects of anatomy relative to which the promontorial and stapedial canals were compared. In order to understand what affects the size of one canal relative to the other, it is necessary to consider what factors affect the scaling of each canal independent of the other.

2. Major aims

Here we rely on recent advances in X-ray micro-computed tomography to quantify the sizes of the promontorial and stapedial canals in a broad comparative sample of primates and other euarchontans. Our analyses of these data have multiple goals. First, we aim to establish an objective and quantitative approach for identifying “reduction” or “enlargement” of branches of the ICA in both living and fossil taxa. Prior studies indicate that the promontorial artery primarily supplies blood to the brain and that

among primates – with the exception of cheirogaleids and lorisiforms – it is aided by only the vertebral artery (Bugge, 1974). Therefore we seek to determine whether promontorial canal absolute diameters vary predictably with endocranial volume (a close proxy for brain mass) or are more closely associated with other variables (body mass or linear measures of cranial size), and whether species with patent promontorial arteries can be distinguished from those with involuted arteries on the basis of promontorial canal cross sectional area relative to endocranial volume. If promontorial canal area is found to correlate strongly with endocranial volume and to distinguish taxa with patent promontorial arteries from those with involuted arteries when considered relative to endocranial volume, then discussions of the "enlargement" and "reduction" of the promontorial canal can be meaningfully and explicitly reframed relative to endocranial volume. Likewise, because the stapedial artery is thought to have an important role in supplying the meninges of the brain (Bugge, 1974; Wible, 1987), it may also have a significant relationship with endocranial volume. Because the stapedial artery is thought to have more interspecifically diverse roles than the promontorial artery (Szalay and Katz, 1973; Bugge, 1974; Wible, 1987), we also explore various other factors that may affect stapedial canal area, including correlations with body mass, linear measures of cranial size, and promontorial canal area.

Second, we seek to re-interpret the functional and systematic significance of variation in the ratio of promontorial canal cross sectional area to stapedial canal cross sectional area among living and fossil primates. In so doing, we consider the effects of intraspecific variation and the scaling factors that influence canal size.

Third, we use Bayesian methods of ancestral state reconstruction to estimate the most likely disposition of the ICA and its branches in the last common ancestor of living primates, as well as the last common ancestor of strepsirrhines, haplorhines, and a number of other less inclusive clades within these groups.

Fourth, we re-assess what the relative sizes of the promontorial and stapedial canals indicate about arterial patency and subordinal phylogenetic affinities in adapiforms and omomyiforms.

3. Institutional abbreviations

AMNH, American Museum of Natural History, New York, New York, USA; BAA, Duke University, Evolutionary Anthropology, Durham, North Carolina, USA; CGM, Egyptian Geological Museum, Cairo, Egypt; CM, Carnegie Museum of Natural History, Pittsburgh, Pennsylvania, USA; DPC, Duke Lemur Center, Division of Fossil Primates, Durham, North Carolina; KNM, National Museums of Kenya, Nairobi, Kenya; FMI, Museo de Fundación Miguel Lillo (Rusconi Collection), Tucuman, Argentina; MACN, Museo Argentino de Ciencias Naturales "B. Rivadavia," Buenos Aires, Argentina; MaPhQ, Montauban Musee d'Histoire Naturelle Victor-Brun, Phosphorites de Quercy locality, Montauban, France; MCZ, Museum of Comparative Zoology, Harvard University, Cambridge, Massachusetts, USA; MPM-PV, Museo Regional Provincial Padre Manuel Jesús Molina, Rio Gallegos, Argentina; NHM-UK, British Museum of Natural History, London, UK; NMB, Naturhistorisches Museum Basel, Basel, Switzerland; SBU, Stony Brook University, Stony Brook, New York, USA; TMM, Texas Vertebrate Paleontology Collections at The University of Texas at Austin, Austin, Texas, USA; UM, University of Michigan Museum of Paleontology, Ann Arbor, Michigan, USA; UM, Université de Montpellier, France; UNSM, University of Nebraska Science Museum, Lincoln, Nebraska, USA; USNM, United States National Museum, Smithsonian Institute, Washington, DC, USA; UW, University of Wyoming, Laramie, Wyoming, USA; UMZC, University Museum of Zoology, Cambridge, UK; YPM, Yale Peabody Museum, New Haven, Connecticut, USA.

4. Materials and methods

4.1. Sample

The sample consists of measurements from 150 specimens representing 77 genera and a similar number of species of extant and extinct euarchontans (Table 1, Supplementary Online Material [SOM] Tables S1–S3). Specifically, 27 of the included species are extinct. Most data were collected from microCT renderings, and the majority of scan data for the extant sample are available through MorphoSource (www.morphosource.org). Data for extant specimens from the MCZ scans originally appeared in Copes and Kimbel (2016) and Copes et al. (2016). These MCZ specimens were scanned at Harvard using the X-Tek HMXST225 μCT scanner. Other material was scanned at the AMNH Microscopy and Imaging Facility, UT Austin's High Resolution X-ray Computed Tomography Center, Duke University's Shared Materials Instrumentation Facility, Penn State's Center for Quantitative imaging, and the Smithsonian Museum of Natural History. One skull of *Adapis parisiensis* (UMZC M538) was scanned at the Imaging and Analysis Centre of the Cambridge University Museum of Zoology. The scan of *Victoriapithecus* (KNM-MB 29100) was generated with the BIR ACTIS 225/300 of the Max Planck Institute for Evolutionary Anthropology, Leipzig, at the time installed at the National Museums of Kenya in Nairobi.

Scanning resolutions were maximized to enable crisp, high fidelity boundaries on carotid canal images. Adequate resolution was more difficult to attain for strepsirrhines (with very small canals relative to head size) than haplorhines. SOM Table S9 provides the resolutions and Morphosource DOI links for all available scans.

4.2. Data collection protocols

MicroCT scans were cropped to include only the petrosal region in order to decrease file size. The files were then segmented in Avizo 8.1 (Visualization Sciences Group, 2009). Segmentation included selecting the space within the main internal carotid canal, the stapedial canal, and/or the promontorial canal when present. Variability in specimen preservation prevented an automated protocol for identifying the boundary between bone and the internal canal space. Typically the segmented versions of the canals were transformed directly into mesh surfaces with no smoothing. Some meshes were smoothed before measurement, but all of these meshes had relatively high resolution (at least 100–200 pixels across the canal diameter). Once the canals were segmented and made into mesh files, the "2d-measurement tool" in Avizo 8.1 was used to measure major and minor diameters of the three different canals, at three different positions (Fig. 2). The major and minor diameters[1] were multiplied to approximate the canal cross-sectional area (SOM Table S1–S3). An error study was executed in which ten specimens representing different major phylogenetic patterns were re-measured on three separate occasions (SOM Table S4): The error on raw measurements was less than 5% in all cases, and the error in computed variables and residuals did not exceed intraspecific ranges of these values.

Differences in the patterns of arterial blood flow among euarchontan taxa (Fig. 1) mandated varying interpretations of the canal measurements. (Fig. 1): In non-cheirogaleid lemuriforms and scandentians, the main trunk of the internal carotid canal is distinguished from its downstream branches because it carries

[1] We originally attempted to take actual cross-sectional areas of segmented canals, but due to differences in data quality and resolution, this proved less precise than measuring two linear diameters.

Table 1
Summary statistics of key variables in arithmetic units.

Taxon	*n*	Sex	BM	PI	BZ	CA	ECV	ICA-m				PA-m				SA-m				SA/PA			
								Mean	Stdev	Max	Min	Mean	Stdev	Max	Min	Mean	Stdev	Max	Min	Mean	Stdev	Max	Min
Piliocolobus badius badius	2	m/f	7850	103.4	77.3	89.4	64.49	6.784	1.602	7.917	5.651	6.784	1.602	7.917	5.651	–	–	–	–	–	–	–	–
Lophocebus albigena	2	m	7890	124.2	74.4	96.1	97.99	4.435	0.310	4.654	4.217	4.435	0.310	4.654	4.217	–	–	–	–	–	–	–	–
Macaca fascicularis	2	f	3884	104.4	71.5	86.4	63.06	4.403	0.216	4.556	4.250	4.403	0.216	4.556	4.250	–	–	–	–	–	–	–	–
Mandrillus leucophaeus	2	m	17,500	201.6	114.4	151.9	160.00	6.318	0.506	6.676	5.960	6.318	0.506	6.676	5.960	–	–	–	–	–	–	–	–
Miopithecus talapoin	3	m	1877	74.1	49.5	60.5	39.08	1.812	0.294	2.008	1.475	1.812	0.294	2.008	1.475	–	–	–	–	–	–	–	–
Nasalis larvatus	1	f	9730	108.4	74.8	90.0	83.84	4.401	–	–	–	4.401	–	–	–	–	–	–	–	–	–	–	–
Papio anubis	2	f	13,300	154.9	92.3	119.6	152.45	7.403	0.469	7.735	7.071	7.403	0.469	7.735	7.071	–	–	–	–	–	–	–	–
Gorilla gorilla gorilla	3	f	71,500	234.0	148.5	186.4	455.89	13.383	1.293	14.357	11.916	13.383	1.293	14.357	11.916	–	–	–	–	–	–	–	–
Homo sapiens	3	m/f	65,000	178.3	131.5	153.1	1422.33	45.560	9.267	55.406	37.009	45.560	9.267	55.406	37.009	–	–	–	–	–	–	–	–
Pongo pygmaeus	3	?	36,948	196.7	127.9	158.6	368.00	12.014	2.844	14.682	9.023	12.014	2.844	14.682	9.023	–	–	–	–	–	–	–	–
Hylobates lar	3	f	5381	101.5	68.3	83.2	100.49	6.853	0.382	7.164	6.426	6.853	0.382	7.164	6.426	–	–	–	–	–	–	–	–
Pan paniscus	3	m/f	37,133	164.1	112.4	135.8	336.28	11.916	0.971	13.011	11.161	11.916	0.971	13.011	11.161	–	–	–	–	–	–	–	–
Alouatta sp.	3	m/f	5753	113.3	76.7	93.2	52.75	3.518	0.935	4.596	2.933	3.518	0.935	4.596	2.933	–	–	–	–	–	–	–	–
Aotus trivirgatus	1	?	989	60.5	38.2	48.0	16.85	1.246	–	–	–	1.246	–	–	–	–	–	–	–	–	–	–	–
Ateles geoffroyi	3	f	7453	107.7	64.9	83.6	106.59	6.841	0.734	7.489	6.044	6.841	0.734	7.489	6.044	–	–	–	–	–	–	–	–
Cacajao rubicundus	1	?	2935	98.9	66.5	81.1	76.00	3.398	–	–	–	3.398	–	–	–	–	–	–	–	–	–	–	–
Callicebus sp.	2	m	1070	61.2	40.4	49.7	17.78	1.373	0.334	1.609	1.137	1.373	0.334	1.609	1.137	–	–	–	–	–	–	–	–
Callithrix jacchus	3	m	318	43.6	29.3	35.7	7.43	0.570	0.040	0.615	0.540	0.570	0.040	0.615	0.540	–	–	–	–	–	–	–	–
Cebuella pygmaea	1	m	110	33.6	22.0	27.2	4.02	0.360	–	–	–	0.360	–	–	–	–	–	–	–	–	–	–	–
Cebus capucinus	2	f	2437	92.5	61.6	75.5	67.02	3.017	0.138	3.114	2.919	3.017	0.138	3.114	2.919	–	–	–	–	–	–	–	–
Chiropotes albinasus	1	f	2132	84.5	53.6	67.3	55.30	2.704	–	–	–	2.704	–	–	–	–	–	–	–	–	–	–	–
Pithecia pithecia	1	?	1760	76.8	51.6	62.9	32.26	1.577	–	–	–	1.577	–	–	–	–	–	–	–	–	–	–	–
Saimiri sciureus	2	m/f	799	64.1	38.6	49.7	24.60	1.430	0.232	1.594	1.267	1.430	0.232	1.594	1.267	–	–	–	–	–	–	–	–
Avahi laniger	2	?	1207	52.8	37.1	44.2	9.86	0.197	0.023	0.213	0.181	0.087	0.008	0.093	0.082	0.060	0.010	0.067	0.053	0.692	0.178	0.819	0.566
Daubentonia madagascariensis	3	m/f	2555	86.4	59.1	71.4	45.31	1.043	0.254	1.204	0.751	0.387	0.129	0.535	0.304	0.577	0.270	0.878	0.357	1.462	0.302	1.640	1.113
Eulemur fulvus ssp.	3	f	2210	91.2	50.1	67.6	23.06	0.543	0.045	0.583	0.494	0.110	0.012	0.123	0.099	0.158	0.052	0.194	0.098	1.418	0.374	1.687	0.991
Hapalemur griseus	2	f	690	64.5	42.5	52.3	14.04	0.340	0.013	0.349	0.331	0.074	0.041	0.103	0.045	0.175	0.023	0.191	0.159	2.714	1.205	3.566	1.862
Indri indri	2	f	6335	103.2	61.1	79.4	35.90	0.557	0.165	0.674	0.440	0.239	0.011	0.247	0.232	0.184	0.069	0.233	0.135	1.328	0.545	0.942	0.584
Lemur catta	3	?	2210	83.1	48.2	63.3	22.90	0.729	0.182	0.907	0.543	0.134	0.048	0.169	0.078	0.291	0.039	0.316	0.246	2.345	0.695	3.139	1.849
Lepilemur sp.	3	m/f	691	53.4	34.9	43.2	8.21	0.074	0.023	0.100	0.058	0.055	0.017	0.073	0.041	0.023	0.018	0.044	0.011	0.389	0.184	0.601	0.280
Prolemur simus	1	?	2150	82.6	58.4	69.5	27.14	0.558	–	–	–	0.121	–	–	–	0.215	–	–	–	1.783	–	–	–
Propithecus sp.	2	?	2955	83.3	55.8	68.2	30.06	0.853	0.309	1.072	0.635	0.130	0.057	0.171	0.090	0.302	0.112	0.381	0.223	2.359	0.177	2.484	2.234
Varecia sp.	3	m/f	3497	105.5	58.8	78.7	32.15	0.699	0.171	0.847	0.512	0.169	0.057	0.204	0.103	0.179	0.053	0.237	0.132	1.263	0.898	2.296	0.664
Microcebus murinus	2	?	65	32.3	20.3	25.6	1.63	0.015	0.002	0.017	0.014	0.022	0.011	0.029	0.014	–	–	–	–	–	–	–	–
Cheirogaleus medius	1	?	140	42.9	29.0	35.3	5.81	0.104	–	–	–	0.095	–	–	–	–	–	–	–	–	–	–	–
Cheirogaleus major	2	m	400	54.9	35.5	44.2	2.60	0.070	0.034	0.094	0.045	0.045	0.000	0.045	0.045	–	–	–	–	–	–	–	–
Mirza coquereli	2	?	312	51.1	31.6	40.2	5.76	0.042	0.012	0.051	0.034	0.042	0.012	0.051	0.034	–	–	–	–	–	–	–	–
Otolemur crassicaudatus	2	m	1170	67.3	44.8	54.9	12.25	0.138	0.074	0.191	0.086	0.124	0.094	0.191	0.058	–	–	–	–	–	–	–	–
Galago senegalensis	3	m	196	43.5	29.2	35.6	3.97	0.027	0.014	0.043	0.017	0.027	0.014	0.043	0.017	–	–	–	–	–	–	–	–
Loris tardigradus	2	?	193	51.4	32.9	41.1	5.87	0.056	0.006	0.061	0.052	0.056	0.006	0.061	0.052	–	–	–	–	–	–	–	–
Nycticebus coucang	2	m	679	55.8	38.3	46.2	11.01	0.120	0.005	0.124	0.117	0.096	0.040	0.124	0.068	–	–	–	–	–	–	–	–
Perodicticus potto	2	m	802	62.0	45.0	52.8	12.81	0.082	0.022	0.098	0.066	0.075	0.032	0.098	0.052	–	–	–	–	–	–	–	–
Galeopterus variegatus	2	m/f	1330	71.1	44.9	56.5	6.78	0.100	0.015	0.110	0.090	0.100	0.015	0.110	0.090	–	–	–	–	–	–	–	–
Cynocephalus volans	3	?	810	68.5	44.3	55.1	5.78	0.122	0.013	0.137	0.115	0.122	0.013	0.137	0.115	0.000	–	–	–	–	–	–	–
Ptilocercus lowii	3	m/f	43	37.3	21.2	28.1	1.67	0.154	0.006	0.158	0.148	0.107	0.021	0.132	0.092	0.092	0.009	0.102	0.085	0.884	0.209	1.031	0.645
Tupaia glis	3	m/f	142	51.0	25.2	35.8	3.00	0.466	0.021	0.489	0.451	0.191	0.042	0.218	0.142	0.175	0.013	0.190	0.166	0.942	0.203	1.166	0.771
Tarsius sp.	4	f	109	39.0	27.4	32.7	3.27	0.323	0.049	0.368	0.265	0.269	0.036	0.307	0.231	0.021	0.007	0.029	0.013	0.083	0.037	0.116	0.043
Megaladapis sp.	1	?	37,703	226.1	102.5	152.2	85.00	1.210	–	–	–	0.806	–	–	–	–	–	–	–	–	–	–	–
Archaeolemur majori	3	?	18,200	136.8	104.2	119.4	93.00	1.071	0.261	1.329	0.807	0.399	0.162	0.508	0.212	0.339	0.141	0.500	0.236	0.933	0.415	1.320	0.496
Babakotia radofilai	2	?	16,000	106.8	76.3	90.3	48.00	0.773	0.148	0.878	0.668	0.357	0.056	0.397	0.317	0.295	0.083	0.353	0.237	0.856	0.367	1.116	0.597
Adapis parisiensis	4	?	1103	81.9	54.5	69.7	8.80	0.599	0.116	0.754	0.474	0.164	0.011	0.175	0.150	0.224	0.048	0.283	0.173	1.385	0.393	1.886	1.003
Cantius ralstoni	1	?	487	–	–	–	–	–	–	–	–	0.168	–	–	–	0.204	–	–	–	1.216	–	–	–
Cantius abditus	1	?	1220	71.5	44.5	56.4	–	–	–	–	–	0.252	–	–	–	0.202	–	–	–	0.801	–	–	–
Cantius nuniensis	1	?	2274	–	–	–	–	–	–	–	–	0.376	–	–	–	0.243	–	–	–	0.646	–	–	–
Leptadapis leenhardti	1	?	6766	94.1	66.6	79.2	10.06	1.823	–	–	–	0.522	–	–	–	0.624	–	–	–	1.196	–	–	–

Notharctus tenebrosus	5	?	2367	77.3	48.1	60.8	7.72	0.840	0.157	1.000	0.673	0.371	0.093	0.477	0.245	0.252	0.034	0.290	0.207	0.707	0.169	0.933	0.576
Smilodectes gracilis	5	?	2585	73.8	50.0	60.6	7.92	1.470	0.324	1.942	1.193	0.607	0.072	0.710	0.535	0.329	0.069	0.420	0.253	0.539	0.068	0.625	0.472
Mahgarita stevensi	1	?	1163	–	–	–	–	–	–	–	–	0.328	–	–	–	0.019	–	–	–	0.057	–	–	–
Parapithecus grangeri	1	?	3373	65.7	53.4	59.2	11.40	1.658	–	–	–	1.658	–	–	–	–	–	–	–	–	–	–	–
Aegyptopithecus zeuxis	2	m/f	4489	83.6	46.9	62.5	17.92	2.371	0.733	2.889	1.852	2.371	0.733	2.889	1.852	–	–	–	–	–	–	–	–
Antillothrix bernensis	1	?	3300	83.0	62.7	72.2	40.58	2.538	–	–	–	2.538	–	–	–	–	–	–	–	–	–	–	–
Dolichocebus gaimanensis	1	?	1554	69.1	38.9	51.8	22.14	1.125	–	–	–	1.125	–	–	–	–	–	–	–	–	–	–	–
Homunculus patagonicus	2	?	2340	72.2	41.4	54.7	19.85	1.288	0.034	1.312	1.264	1.288	0.034	1.312	1.264	–	–	–	–	–	–	–	–
Tremacebus harringtoni	1	?	1600	–	–	–	16.35	1.969	–	–	–	1.969	–	–	–	–	–	–	–	–	–	–	–
Tetonius homunculus	1	?	84	–	–	–	1.50	–	–	–	–	–	–	–	–	–	–	–	–	–	–	–	–
Omomys carteri	1	?	377	42.5	28.9	35.1	–	np	–	–	–	0.089	–	–	–	0.095	–	–	–	1.068	–	–	–
Microchoerus erinaceus	1	?	373	49.5	34.3	41.2	4.26	0.463	–	–	–	0.199	–	–	–	0.152	–	–	–	0.767	–	–	–
Necrolemur antiquus	1	?	267	41.0	26.0	32.6	3.80	0.356	–	–	–	0.227	–	–	–	0.183	–	–	–	0.805	–	–	–
Victoriapithecus macinnesi	1	?	6000	112.5	74.7	91.6	35.60	2.706	–	–	–	2.706	–	–	–	0.000	–	–	–	–	–	–	–
Rooneyia viejaensis	1	?	437	50.6	36.5	42.9	7.23	0.565	–	–	–	0.335	–	–	–	0.075	–	–	–	0.225	–	–	–
Ignacius graybullianus	1	?	286	48.2	35.3	41.3	2.14	0.029	–	–	–	0.029	–	–	–	–	–	–	–	–	–	–	–
Microsyops annectens	1	?	1863	78.0	42.0	57.2	5.90	0.342	–	–	–	0.255	–	–	–	0.070	–	–	–	0.275	–	–	–
Shoshonius cooperi	1	?	105	28.2	21.9	24.8	–	–	–	–	–	0.145	–	–	–	0.083	–	–	–	0.575	–	–	–
Afradapis longicristatus	2	?	1805	–	–	–	–	–	–	–	–	0.397	0.080	0.454	0.340	0.256	0.076	0.309	0.202	0.677	0.328	0.909	0.445
Carpolestes simpsoni	1	?	100	39.6	23.4	30.5	–	0.281	–	–	–	0.023	–	–	–	0.160	–	–	–	7.111	–	–	–

Abbreviations: BM – body mass (units of grams), CA – cranial area = square root taken after multiplying prosthion-inion length by bizygomatic breadth (units of millimeters), ECV – endocranial volume (units of cubic centimeters), ICA-m – mean value of Internal Carotid Canal Area (average of prox, mid, and dist values) (units of square millimeters), PA-m – mean value of promontorial canal area (units of square millimeters), SA-m mean value of stapedial canal area (units of square millimeters). SA/PA – value of SA-m divided by PA-m.

blood destined for the stapedial canal and blood and/or nerves destined for the promontorial canal. In contrast, the main carotid canal (starting with the posterior carotid foramen) is not distinct from its downstream segments in cheirogaleids, lorisiforms, dermopterans, and anthropoids because of the absence of the stapedial system in these taxa. In non-anthropoids lacking the stapedial artery, all that is consistently measureable is a canal leading into the tympanic cavity (traveling through the posterior septum): a transpromontorial canal is never present, though in some instances the anterior carotid foramen is measurable. In anthropoids, a distinct canal runs from the posterior carotid foramen to the endocranial space. Our data collection protocol therefore equates the promontorial canal of non-cheirogaleid lemuriforms, scandentians and other taxa with similar anatomy (e.g., many fossil primates), to the posterior carotid canal in cheirogaleids, lorisiforms, and dermopterans, and to the entire internal carotid canal of anthropoids. Thus, in non-cheirogaleid lemuriforms, scandentians, and tarsiers there are always three sets of canal measurements. In cheirogaleids, lorisiforms and dermopterans there can be either one or two sets of distinct measurements (two sets if the anterior carotid canal is enclosed and measureable). In anthropoids, there is always just one set of distinct measurements (SOM Table S1).

To understand better what drives variation in the dimensions of the carotid canal, we compared our measurements to datasets on species mean body mass, endocranial volume, and cranial dimensions for the same taxa (Table 1, SOM Tables S2 and S3). For extant taxa, the majority of values for both body mass and endocranial volume were taken from supplementary files of Isler et al. (2008). For non-primate euarchontans, we reference Stephan et al. (1981), Pirlot and Kamiya (1982) and Tacutu et al. (2013). For fossil taxa, we cite body mass and endocranial volumes reported in Radinsky (1979), Martin (1990), Godfrey and Jungers (2002), Bush et al. (2004), Simons et al. (2007), Silcox et al. (2009a,b, 2010), Catlett et al. (2010), Kay et al. (2012), Kirk et al. (2014), Gonzales et al. (2015), Ramdarshan and Orliac (2015), and Harrington et al. (in press). For some fossil taxa, we employed the species' means of body mass predictions based on calcaneal dimensions reported in Boyer et al. (2013). For several others (*Afradapis*, *Parapithecus*, *Mahgarita*, and *Aegyptopithecus*) the computation of body mass was more involved and is described in the supplemental methods section (SOM Part I). Several taxa were lacking published endocranial volumes and we generated these ourselves (*Cynocephalus volans* and *Ptilocercus lowii*). Data sources on a per specimen basis are given in SOM Table S2.

Finally, as a proxy for head size, "cranial area" was computed as the square root of the product of prosthion-inion length and bizygomatic breadth. These values were associated with individual specimens using sex-specific means from an unpublished dataset collected by ECK (Table 1, SOM Tables S1–S3). In some cases where measurements were not already available for a particular species, we went back to the specimens from which we obtained canal diameters and took cranial measurements on the same individual. Finally, for most fossils, the canal measures and cranial measures come from the same specimen. Case specific sources of cranial data are given in SOM Table S2.

4.3. Phylogenetic framework

In order to analyze patterns of variance statistically, we needed to use methods that take into account the fact that data points from different individuals and species are interdependent due to phylogenetic relatedness. Phylogenetic interdependence arises through autocorrelation, such that closely related sister taxa are expected to be more similar to one another than more distantly related forms (Nunn, 2011). Estimating and correcting for

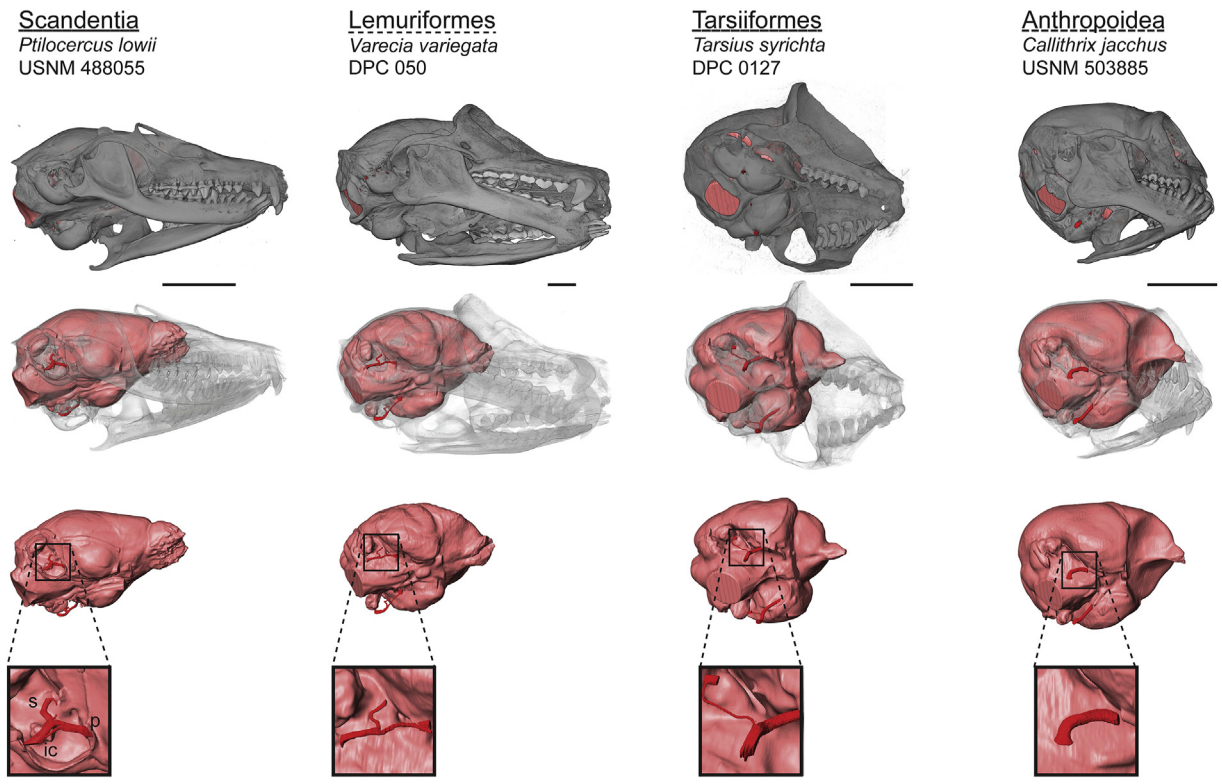

Figure 1. Internal carotid patterns among euarchontans. In this study we use microCT scans to quantify internal anatomy of the skull and its scaling among living euarchontans. The approximate size of various soft tissue structures can be inferred from bony structures that encase them. In this study, we were interested specifically in using endocranial volume (pink) as a proxy for brain size, and the diameters of the bony canals that transmitted the branches of internal carotid neurovasculature (red) as a proxy for the size of the arteries that once occupied them. The taxa shown in the figure are exemplars for most of the major anatomical patterns observed in this study (patterns omitted from this image, but included in the study, include those of dermopterans, cheirogaleids, and lorisiforms, in which none of the major branches of the internal carotid artery persists into adulthood). Skulls are scaled to roughly similar endocranial volumes. From top to bottom, each exemplar is represented by an opaque rendering of a microCT dataset of a skull or cranium in ventrolateral view, then a translucent version of the same dataset showing the positions and morphology of the endocranial and internal carotid endocasts relative to the skull, then an unobstructed view of both endocasts, and finally a 300% zoom in on the internal carotid casts. In the bottom image, the red branch extending up and to the left is the stapedial artery canal endocast (s). The branch extending to the right is the promontorial branch (p). The branch extending downward to the left is the internal carotid main stem (ic). Note that in *Callithrix* (far right) the promontory branch is not typically distinguishable from the main stem of the internal carotid because of the lack of a stapedial branch. Note the relative size differences of the promontorial arteries of these four taxa. Our measurements (as shown in Fig. 2) allowed us to demonstrate this variation quantitatively (see text, tables and Figs. 3–5). Scale bar is 10 mm. (For interpretation of the references to color in this figure legend, the reader is referred to the web version of this article.)

phylogenetic autocorrelation requires an explicit hypothesis of the pattern and timing of divergence among the taxa analyzed. Since no existing character matrix or published phylogeny includes all the taxa sampled here, we compiled existing phylogenetic trees into a single tree to use in our statistical analyses. This compilation was done using an MRP supertree approach (Ragan, 1992) following the methods used by Boyer et al. (2013, 2015). All trees used in analyses of this study are provided as nexus format within SOM Part II.

We constructed our trees by first conducting two phylogenetic analyses (one using parsimony, in PAUP 4.0b10, the other using Bayesian inference, in MrBayes v. 3.2.5) to generate 'base' trees that include the majority of the early fossil primates for which canals could be measured. The character matrix for these analyses was a modified version of that published by Seiffert et al. (2015). We modified it specifically by redefining and recoding several characters relating to cranial circulation based on some of the results of this study (SOM Part III) and by re-scoring the middle Eocene primate *Rooneyia viejaensis*, taking into account high-resolution micro-CT scans of the single known specimen (Kirk et al., 2014). Branch lengths for fossils were set according to the protocol used in Boyer and Seiffert (2013) and Boyer et al. (2013, 2015). Additional information on the source trees for the MRP analysis, and the ages of fossil taxa, are provided in SOM Part IV. The results of the two analyses of the "core" matrix encompass a range of competing views on the phylogenetic position of early fossil primates: The Bayesian analysis recovers Eocene adapiforms as paraphyletic with respect to crown strepsirrhines, and Eocene omomyiforms as paraphyletic with respect to a "strict" tarsier-anthropoid clade (MacPhee and Cartmill, 1986; Ross, 1994), whereas the parsimony result places omomyiforms with tarsiers to the exclusion of anthropoids (Szalay, 1975) and places adapiforms as a monophyletic (rather than paraphyletic) sister group of living strepsirrhines. In the supplementary document (SOM Part V), we discuss the result of adding *R. viejaensis* to the character-taxon matrix.

4.4. Statistical analyses

We designed an analytical workflow to address the major aims of this study as described in the introduction. This workflow (or framework) is described in detail in the next methods' section, "Analytical framework". The present section provides more general information on data transformation, analysis types, and software packages utilized.

All data were natural log transformed prior to analysis. All analyses were run on species' means. We used both phylogenetically informed and conventional statistics to evaluate correlations and associations in our data. Conventional procedures were used whenever measures of phylogenetic signal (Pagel's λ) were

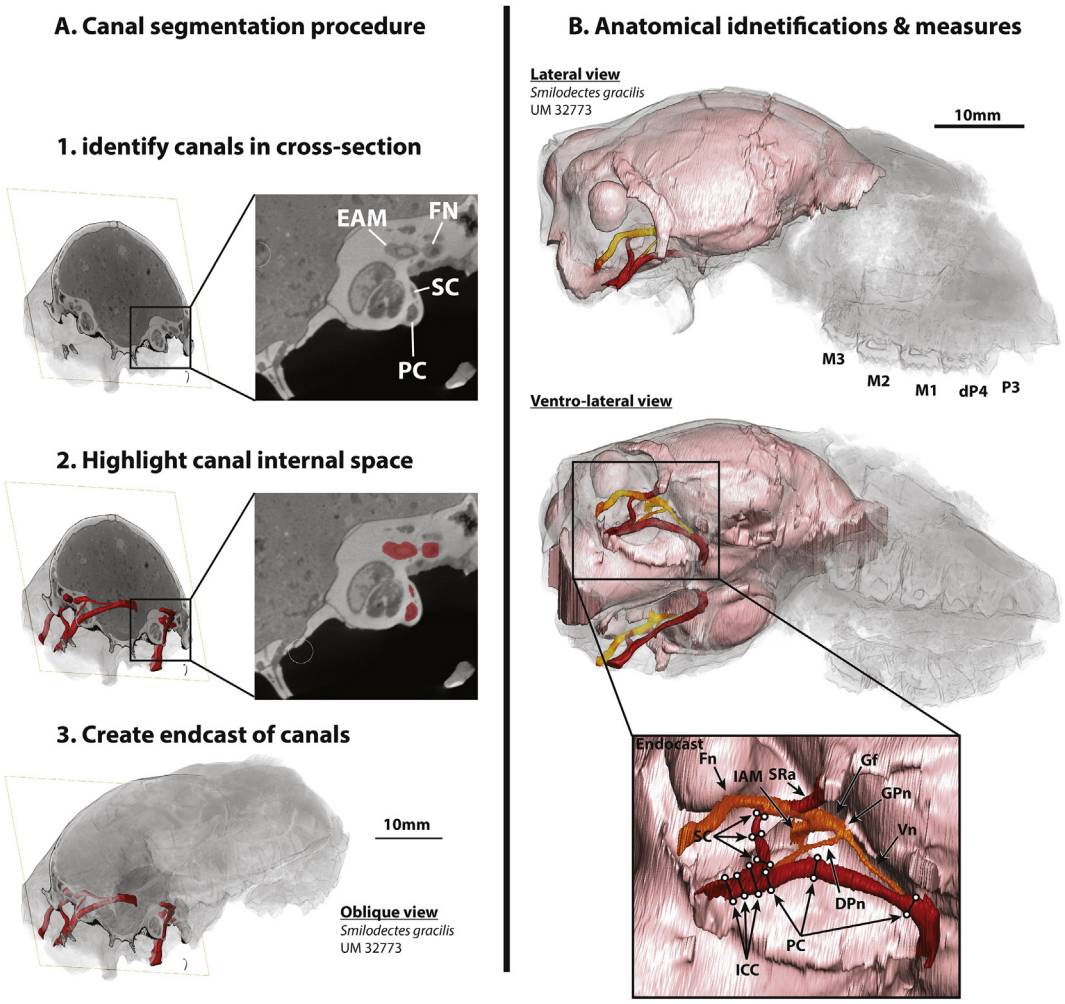

Figure 2. Creating, identifying, and measuring endocasts of neurovasculature. We use the comparative extant data (see visualizations in Fig. 1) in interpretations of fossils like the notharctid adapiform shown here. Though this particular fossil is a juvenile by dental standards, previous studies show it to have a fully adult-sized endocast (Harrington et al., in press). Measurements include major and minor diameters of the stapedial artery canal (SC), the promontory artery canal (PC) and the internal carotid main stem canal (ICC). Other tube-like passages that intersect and are confluent with these spaces include those carrying branches of the facial nerve and internal carotid nerve (shown in yellow-orange). Remaining abbreviations: DPn – canal for the deep petrosal branch of the internal carotid nerve; Fn – canal for the facial nerve (cranial nerve VII), Gf – canal for genu facialis, GPn – canal for greater petrosal nerve of facial nerve; IAM – internal acoustic meatus; SRA – canal for superior ramus of stapedial artery (to merge with groove for petrosquamous sinus) Vn – canal for vidian nerve (= nerve of pterygoid canal).

nonsignificant (i.e., when the maximum likelihood value of Pagel's λ is not distinguishable from zero). We used Caper (Orme et al., 2012) in R coding language to run phylogenetically generalized least squares (PGLS) regressions with either promontorial canal area, stapedial canal area or stapedial-promontory canal ratio as the dependent variable. Regressions using either one or multiple independent variables were run. When multiple regressions were run, we also assessed multi-colinearity of the independent (explanatory) variables with Tolerance and Variance Inflation Factors (O'Brien, 2007). Caper was also used to run phylogenetically informed t-tests evaluating whether taxa with a consistently patent promontorial artery have a smaller ratio of stapedial canal area to promontorial canal area than taxa that frequently have an involuted promontorial artery.

Though four different NEXUS files (SOM Part II) are used to represent tree topology in the various statistical analyses of the data, these NEXUS files differ only in taxonomic inclusion (depending on the sample available for each analysis). All four are equivalent in topology and reflect the MRP tree based on the core tree resulting from maximum parsimony analysis (SOM Figs. S1 and S2).

To determine whether having a consistently present promontorial artery (versus variably present or involuted) affected the scaling relationship between canal cross section and endocranial volume, we used Phylogenetic Analysis of Covariance (PhyANCOVA) in BayesTraitsV2 (Pagel and Meade, 2013). Trees 6–7 were used for these analyses (SOM Part II). Conventional regression analyses were run in PAST (Hammer et al., 2006).

4.5. Analytical framework

4.5.1. Correlates of promontorial canal area In order to reframe the issue of ICA enlargement and reduction in a biologically meaningful, quantitative context, we first addressed the question of whether arterial canal area is tied closely to endocranial volume, body mass, or head size (as defined in previous sections). We ran a phylogenetic multiple regression of promontorial canal area (dependent variable) against body mass, endocranial volume, and cranial area (independent variables) using Caper (Orme et al., 2012) in R coding language (Table 2, equation #4). We also calculated the bivariate correlations of each of the independent variables against

promontorial canal area separately (Table 2, equations #1–3). These analyses utilize tree #3 (SOM Part II).

Each predictor variable used in multiple regression was assessed for multicollinearity with the other predictors by treating it as a dependent variable and regressing it against the remaining predictor variables (SOM Table S5). Because we found substantial degrees of multicollinearity among predictor variables, we carefully considered the importance of each predictor variable based on 1) whether it describes a significant amount of variance in multiple regression with other predictors, 2) whether it is significant in a bivariate context, and 3) whether it explains more or less variance than other predictors in a bivariate context with promontorial canal area.

It should be noted that multicollinearity does not formally invalidate multiple regression unless the correlation among predictor variables is perfect (correlation coefficient = 1.0). However, slightly lower degrees of multicollinearity can apparently make the pattern of significance of multiple regression less tractable when predictor variables are removed or added. A typical rule of thumb is that levels of multicollinearity should have a tolerance below 0.10 (tolerance = $1 - r^2$) or a variance inflation factor (VIF) below 10 (VIF = 1/tolerance) (O'Brien, 2007). Only two variables in one set of regressions exceed this threshold (SOM Table S5). It appears that previously suggested alternatives to multiple regression have statistical effects that may be worse than using a multiple regression with mutually correlated predictors (O'Brien, 2007).

The interpretation of a multiple regression coefficient for a given variable is valid regardless of the presence of multicollinearity: it is the effect of that predictor variable on the dependent variable when the other variables are held constant. This effect should be significant if it is independent of variance in other predictor variables. When a predictor variable is significant in a bivariate context, but not in a multivariate context, we interpret that to mean that its bivariate effects are better ascribed to other predictor variables with which it covaries.

4.5.2. Effects of artery involution on relative promontorial canal area The next question we evaluated was whether species with patent promontorial arteries can be distinguished from those with consistently or frequently involuted arteries on the basis of relative promontorial canal area. We conducted a phylogenetic ANCOVA (PhyANCOVA) using BayestraitsV2 (Pagel and Meade, 2013) based on Tree #6 (SOM Part II). As with our other comparative methods, only species' mean values were used. ANCOVA allows assessment of whether two or more groups exhibit different scaling relationships of a response variable (promontorial canal area) to a covariate (endocranial volume, body mass, or cranial area). The scaling relationships may differ by slope or (if slopes are not different) by intercept. We structured our analysis to test for slope and intercept differences among three groups of extant taxa in our sample: 1) taxa with a consistently patent promontorial artery, 2) taxa with a condition similar to non-cheirogaleid lemuriforms in which the promontorial artery may be frequently or consistently involuted while the stapedial canal is consistently present, and 3) taxa with a condition like cheirogaleids and lorisiforms in which both branches of the internal carotid artery are involuted. We also assessed whether it was most likely that our taxa fall into the three categories as stated above, versus two categories or a single category. This assessment was done using BayestraitsV2 to calculate the log likelihood of each ANCOVA model. These likelihoods were compared using a chi square test in which the degrees of freedom are equal to the difference in complexity of the models being compared. Complexity of a model is given by the number of parameters estimated by the analysis. So, for example, in the case of an analysis in which the data are represented by three groups, and in which distinct slopes and intercepts are estimated for each group, there are six estimated parameters. In an analysis with three groups, but in which a single slope is assumed to characterize all three groups, there are only four parameters to estimate. Thus the difference in complexity between these two models (and the degrees of freedom for chi square) is two.

In order to determine the most statistically justifiable treatment for these groups we modeled the data in five different ways, varying the number of separate scaling relationships from one to three groups (A = one group, all taxa, B = two groups, promontorial reliant vs. non-reliant, C = three groups, promontorial reliant, vs. non-reliant with stapedial, vs. non-reliant without stapedial) (Table 4). For each set of models with more than one group, we ran a version that assumed equal slopes among groups and one that allowed slopes to vary. We then compared the likelihoods of all models with different numbers of parameters and chose the model with the highest likelihood that was significantly different from less complex models with lower likelihoods (Table 5).

4.5.3. Incorporating fossils for a more robust assessment of effects of promontorial artery involution Because our PhyANCOVA affirmed that taxa with a consistently patent promontorial artery are distinguishable from those with a frequently or consistently involuted artery (see Results), we computed prediction confidence intervals on the regression including those taxa with a consistently patent promontorial artery (Table 2, equation #5). These prediction intervals allowed us to use promontorial canal area and endocranial volume to infer which fossils are likely to have had a patent promontorial artery (Table 6). We then ran a second PhyANCOVA that incorporated fossil taxa. In this analysis, all fossils with sufficiently large promontorial canals were placed in the promontorially "reliant" group; fossils with a relatively small promontorial canal were coded as representing one of two other groups depending on whether they were observed to have an ossified stapedial canal or not. A "sufficiently large promontorial canal" was defined as one with an area that is above the lower 95% prediction confidence intervals of the relationship for extant taxa with consistently patent arteries. A "relatively small canal" was defined as one with an area that is below the lower 95% prediction interval of the relationship for extant taxa with consistently patent arteries. Prediction confidence intervals of a regression were computed using equation 17.29 of Zar (1984). Adding new taxa to a Bayestraits analysis required utilizing a new tree that also includes those taxa. Thus a second iteration of phylogenetic ANCOVA utilizing fossil taxa used tree #7 (SOM Part II).

4.5.4. Revisiting multiple regression based on ANCOVA results Because the most inclusive version of our PhyANCOVA shows that different promontorial groups have significantly different scaling relationships (see Results), it was necessary to reassess the best correlate of promontorial canal area within each group (i.e., body mass, endocranial volume, or head size) (Table 2, equations #6–14).

4.5.5. Correlates of stapedial canal area In order to reframe the question of stapedial canal enlargement and reduction, we took a similar approach to that pursued for promontorial canal size. We ran multiple and bivariate phylogenetic regressions with stapedial canal area as the dependent variable and endocranial volume, body mass, cranial area, and promontorial canal area as the independent variables (Table 3, equations #15–23). One might question why stapedial canal area was not tested as one of the independent variables potentially driving promontorial canal area in earlier analyses. The reason we did not do this test is that the stapedial canal has a more limited taxonomic distribution than the promontorial canal, which reveals *a priori* that stapedial canal area cannot drive promontorial canal area as a general rule.

However, in the sub-sample of taxa with a visible and measureable stapedial canal, a promontorial canal or its equivalent can always be measured. Therefore the promontorial artery could conceivably explain variance in stapedial canal size.

We ran multiple phylogenetic regression analyses on a subsample of taxa with ECV data. This subsample included all those taxa with a measurable stapedial canal or groove (Table 3, equation #19).

We also ran multiple and bivariate phylogenetic regression analyses on a slightly expanded sample by dropping ECV from the variable list and using data for all taxa for which we had at least promontorial canal area, stapedial canal area, body mass and head size (Table 3, equations #23). This analysis used tree #1, which differs from tree #3 (as well as from #6–7) in having additional fossil taxa for which endocranial volume is not available (SOM Part II). We again assessed multicollinearity among variables in multiple regression.

4.5.6. Re-assessing the ratio of promontorial canal area to stapedial canal area Although prior research has inferred the presence of a patent promontorial artery from the ratio of promontorial and stapedial canal sizes (Gingerich, 1973, 2012), it is not clear whether the ratio is generally informative for such inferences. We tested whether the ratio of stapedial canal area and promontorial canal area (SA/PA) was associated with promontorial artery patency with a phylogenetic t-test, again using Caper implemented in the R coding language. As for the multiple regression analyses looking at correlates of stapedial canal area, we utilized a subset of the total sample. Also excluded were any additional fossil taxa that could not be classified as having had patent promontorial arteries (due to lack of associated endocranial volume) in the preceding analyses.

Another test of whether SA/PA is indicative of promontorial patency was conducted by regressing SA/PA against promontorial canal area, represented as a residual from its regression against endocranial volume in the full sample (Table 2: equation #1). If SA/PA reflects promontorial arterial patency, it should correlate inversely with the residual of promontorial canal area relative to endocranial volume. We assessed this once again with phylogenetic generalized least squares and with the subsample including only taxa with stapedial canals (Table 3, equation #24).

Finally, if a larger stapedial than promontorial canal is a clear indicator of strepsirrhine phylogenetic affinities in fossil taxa (Gingerich, 1973; Szalay, 1975; MacPhee and Cartmill, 1986; MacPhee et al., 1988; Gingerich, 2012), then we expect all extant strepsirrhines to have SA/PA ratios greater than 1.0. Similarly, if a smaller stapedial than promontorial canal is a clear indicator of haplorhine phylogenetic affinities in fossil taxa, then we expect all extant haplorhines to have SA/PA ratios less than 1.0. We report intraspecific ranges of the SA/PA ratio in Table 1.

4.5.7. Modeling character evolution and ancestral state reconstruction (ASR) We estimated ancestral values of absolute stapedial canal area, promontorial canal area and endocranial volume for 14 different euarchontan clades to determine which character states are most likely derived and which are primitive (Table 7). Using BayesTraitsV2, the first step in ASR was to test different models of character evolution for each of the three variables. Once we determined the best-fitting model of evolution (i.e., random walk, or random walk with a directional trend) and phylogenetic scaling parameters (i.e., none, delta, kappa, or lambda) for each variable, we then used that model to estimate ancestral states at the following nodes on both Bayesian and parsimony-based trees: 1) Primatomorpha, 2) Euprimates, 3) Adapiformes + Strepsirrhini, 4) crown Strepsirrhini, 5) crown Lorisiformes, 6) crown Lemuriformes, 7) non-*Daubentonia* lemuriforms, 8) crown Cheirogaleidae, 9) crown Haplorhini (which includes omomyiforms on the parsimony "core" trees [Trees #1, #3, #7], but not on the Bayesian "core" trees [Trees #2, #4]), 10) crown Anthropoidea, 11) Platyrrhini + *Homunculus* and other stem platyrrhines, 12) crown Catarrhini, 13) crown Cercopithecoidea + *Victoriapithecus*, and 14) Hominoidea. Marginal likelihoods were estimated from 50 million generation-long MCMC chains to compute log Bayes factors. Complex models were favored over simpler models only if log Bayes factors were >2 (Pagel and Meade, 2013). In addition, ancestral values at the node that includes omomyiforms + crown haplorhines were estimated on the Bayesian "core" trees (Trees #2 & #4). All ancestral estimates were based on the combined results of two independent, 50 million generation MCMC chains; all provided strong evidence for convergence of likelihood estimates.

We assessed promontorial reliance at ancestral nodes by plotting estimated promontorial canal area against estimated endocranial volume and assessing whether the points fell within the range of variation for extant and fossil taxa thought to be promontorially reliant. We took the same approach with SA/PA, reconstructing stapedial canal area and promontorial canal area separately in order to then compute SA/PA for ancestral nodes.

5. Results

5.1. Correlates of promontorial canal area

Phylogenetic generalized least squares regressions of promontorial canal area against endocranial volume, head size (=cranial area), and body mass were all highly significant when tested separately (Table 2, equations #1–3). The highest correlations were with endocranial volume, followed by cranial area, and finally body mass. Interestingly, promontorial canal area was found to be strongly positively allometric with respect to endocranial volume (slope>>0.66) (Table 2, equation #1; Fig. 3), isometric with respect to cranial "area" (which is actually a 'linear' variable, thus an isometric slope is ~2.0) (Table 2, equation #2), and negatively allometric with respect to body mass (slope<<0.66) (Table 2, equation #3).

However, phylogenetic multiple regression of promontorial canal area against body mass, endocranial volume, and cranial area on the full sample of 65 specimens shows that only endocranial volume correlates significantly with promontorial canal area (Table 2, equation #4) when holding other variables constant. None of the variance inflation factors (VIF) exceeds 10, suggesting that multicollinearity of predictor variables is not a concern (SOM Table S5).

5.2. Effects of artery involution on relative promontorial canal area

Having determined that endocranial volume is the only significant correlate of promontorial canal area when controlling for effects of body mass and cranial area, we ran PhyANCOVAs to determine whether species with patent promontorial arteries can be distinguished from those with consistently or frequently involuted arteries on the basis of relative promontorial canal area (Table 4).

We compared the likelihoods of all models with different numbers of parameters from Table 4 and found the most likely model to be one in which there are three groups (#1 – promontorially patent, #2 – promontorially defunct in combination with a stapedial canal, and #3 – promontorially defunct with no trace of any patent arterial branches of the ICA) with different intercepts, but the same slope (Table 5). This result is consistent with patterns of significance in post hoc comparisons of slopes and intercepts between groups in Table 4. That is, none of the slopes of groups 1–3 was ever found to be significantly different, but in all models that

Table 2
Regression analyses of promontorial canal area (dependent) on potential explanatory variables.

#	Tree*	Independent Var.	ʎ	*n*	df	Int.	Int. SE	Int. CI	Int. *p*	B1	B1 SE	B1 CI	B1 *p*	B2	B2 SE	B2 *p*	B3	B3 SE	B3 *p*	B4	B4 SE	B4 *p*	m-r2	adj-r2
Regressions of full sample; promontorial canal area (PA) is the dependent variable**																								
1	3	ECV	0.863	66	64	−3.108	0.335	0.669	<0.0001	0.809	0.074	0.148	<0.0001	–	–	–	–	–	–	–	–	–	0.65	0.65
2	3	CA	0.848	65	63	−9.768	0.930	1.858	<0.0001	2.060	0.225	0.450	<0.0001	–	–	–	–	–	–	–	–	–	0.57	0.56
3	3	BM	0.848	66	64	−5.004	0.561	1.120	<0.0001	0.491	0.065	0.129	<0.0001	–	–	–	–	–	–	–	–	–	0.47	0.47
4	3	BM, ECV,CA	0.884	65	61	−4.510	1.338	–	0.001	0.113	0.082	–	0.174	0.624	0.144	<0.0001	0.250	0.422	0.56	–	–	–	0.68	0.67
Regressions of extant sample in which promontorial arteries are consistently present; PA is the dependent variable																								
5	3	ECV	0.000	26	24	−2.336	0.121	0.249	<0.0001	0.854	0.029	0.059	<0.0001	–	–	–	–	–	–	–	–	–	0.97	0.97
Regressions of full sample in which promontorial arteries are consistently present*; PA is the dependent variable**																								
6	3	ECV	0.000	40	38	−2.517	0.129	0.261	<0.0001	0.903	0.037	0.075	<0.0001	–	–	–	–	–	–	–	–	–	0.94	0.94
7	3	ECV	NA	40	38	−2.429	0.125	0.253	–	0.881	0.034	0.068	–	–	–	–	–	–	–	–	–	–	–	0.95
8	3	CA	0.744	39	37	−9.108	0.985	1.997	<0.0001	2.061	0.243	0.492	<0.0001	–	–	–	–	–	–	–	–	–	0.66	0.65
9	3	BM	0.809	40	38	−3.929	0.740	1.497	<0.0001	0.412	0.090	0.183	<0.0001	–	–	–	–	–	–	–	–	–	0.35	0.34
10	3	BM, ECV,CA	0.000	39	35	−1.930	0.989	–	0.06	−0.018	0.072	–	0.81	0.964	0.084	<0.0001	−0.159	0.351	0.65	–	–	–	0.95	0.94
Regressions of full sample in which promontorial arteries are consistently absent or variably present*; PA is the dependent variable**																								
11	3	ECV	0.978	26	24	−4.050	0.267	0.552	<0.0001	0.833	0.076	0.156	<0.0001	–	–	–	–	–	–	–	–	–	0.84	0.83
12	3	CA	0.000	26	24	−10.999	0.813	1.678	<0.0001	2.155	0.201	0.416	<0.0001	–	–	–	–	–	–	–	–	–	0.83	0.82
13	3	BM	0.000	26	24	−6.111	0.391	0.807	<0.0001	0.542	0.055	0.113	<0.0001	–	–	–	–	–	–	–	–	–	0.80	0.79
14	3	BM, ECV,CA	0.000	26	22	−8.480	1.604	–	<0.0001	−0.109	0.194	–	0.579	0.416	0.145	0.01	1.472	0.659	0.04	–	–	–	0.88	0.86

*See supplementary information and SOM Figs. S1–S2 for tree numbers. Pagel's ʎ values followed by asterisk are not significantly distinguished from zero. **Samples including CA differ from those lacking it by not including data on *Tremacebus*, the skull of which is too incomplete. ***Fossil taxa are included based on whether they plot above or below the lower prediction confidence interval of regression #5.
Abbreviations: # – reference number of regressions used in text, CI – 95% confidence limits, SA – stapedial canal area, ECV – endocranial volume, BM – body mass, PA, promontorial canal area, PA-res – residual PA from that predicted from regression of PA on ECV (based on sample of equation #1, but with slightly different coefficients due to an error in updating datasets during data preparation: Int = 3.097, B1 = 0.809), Int. – intercept, B1 -– first coefficient in multiple regression or 'slope' of single regressions, B2-4 subsequent coefficients in multiple regression (note that coefficients correspond to independent variables in order listed), SE – standard error of estimate, *p* – probability, *n* – sample size, df – degrees of freedom.
Pagel's ʎ – parameter representing strength of phylogenetic signal with a maximum of around 1 (strong signal) and minimum of 0 (no signal).

Table 3
Regression analyses of stapedial canal area (dependent) on potential explanatory variables.

#	Tree*	Independent Var.	ʎ	*n*	df	Int.	Int. SE	Int. CI	Int. *p*	B1	B1 SE	B1 CI	B1 *p*	B2	B2 SE	B2 *p*	B3	B3 SE	B3 *p*	B4	B4 SE	B4 *p*	m-r2	adj-r2
Regressions of full sample with a stapedial canal, and data on endocranial volume, body mass, and cranial area; stapedial canal area (SA) is the dependent variable																								
15	3	BM	1.000	23	21	−5.189	0.788	1.639	<0.0001	0.473	0.088	0.182	<0.0001	–	–	–	–	–	–	–	–	–	0.58	0.56
16	3	ECV	0.808	23	21	−3.151	0.566	1.176	<0.0001	0.678	0.232	0.482	0.008	–	–	–	–	–	–	–	–	–	0.29	0.26
17	3	PA	1.000	23	21	−0.808	0.488	1.015	0.113	0.871	0.127	0.265	<0.0001	–	–	–	–	–	–	–	–	–	0.69	0.68
18	3	CA	0.597	23	21	−8.514	2.002	4.162	<0.0001	1.693	0.511	1.063	0.003	–	–	–	–	–	–	–	–	–	0.34	0.31
19	3	BM, ECV, PA,CA	0*	23	18	−5.785	3.090	–	0.08	−0.337	0.206	–	0.12	0.232	0.321	0.48	0.670	0.286	0.03	1.725	0.939	0.08	0.53	0.43
Regressions of full sample with a stapedial canal, and data on body mass, and cranial area; SA is the dependent variable																								
20	1	BM	0.967	27	25	−4.109	0.707	1.457	<0.0001	0.344	0.091	0.186	0.0008	–	–	–	–	–	–	–	–	–	0.37	0.34
21	1	PA	0.988	27	25	−0.832	0.572	1.177	0.158	0.598	0.139	0.286	0.0002	–	–	–	–	–	–	–	–	–	0.43	0.40
22	1	CA	0.646*	27	25	−6.621	1.531	3.153	0.0002	1.238	0.403	0.831	0.005	–	–	–	–	–	–	–	–	–	0.27	0.24
23	1	BM, PA,CA	1.000	27	23	−6.86904	1.83841	–	0.001	−0.23361	0.1964	–	0.246	0.162	0.186	0.394	1.770	0.253	0.021	–	–	–	0.40	0.31
Regressions of full sample with a stapedial canal and for which endocranial volume is also available, with the ratio of SA to PA (SA/PA) as the dependent variable																								
24	3	PA-res	1.000	23	21	−0.547	0.444	0.922	0.23	−0.219	0.139	0.288	0.13	–	–	–	–	–	–	–	–	–	0.11	0.06

*See supplementary information and SOM Figures S1–S2 for tree numbers. Pagel's ʎ values followed by asterisk are not significantly distinguished from zero.
Abbreviations: # – reference number of regressions used in text, CI – 95% confidence limits, SA – stapedial canal area, ECV – endocranial volume, BM – body mass, PA, promontorial canal area, PA-res – residual PA from that predicted from regression of PA on ECV (based on sample of equation #1, but with slightly different coefficients due to an error in updating datasets during data preparation: Int. = 3.097, B1 = 0.809), Int. – intercept, B1 – first coefficient in multiple regression or 'slope' of single regressions, B2-4 subsequent coefficients in multiple regression (note that coefficients correspond to independent variables in order listed), SE – standard error of estimate, *p* – probability, *n* – sample size, df – degrees of freedom.
Pagel's ʎ – parameter representing strength of phylogenetic signal with a maximum of around 1 (strong signal) and minimum of 0 (no signal).

Table 4
Phylogenetic ANCOVAs to determine number of distinct scaling relationships between promontory canal cross sectional area and endocranial volume.

n/grp	S#	ʎ	r2	log(L)	Intercepts						Slopes						Post hoc comparisons (*p*-value of identity)						
					Int1	Int1 SE	Int2	Int2 SE	Int3	Int3 SE	S1	S1 SE	S2	S2 SE	S3	S3 SE	Int1v2	Int2v3	Int1v3	S1v2	S2v3	S1v3
Extant only (Tree #6)																						
(47,0,0)	1	1	0.81	−19.683	−3.141	0.323	–	–	–	–	0.806	0.056	–	–	–	–	–	–	–	–	–	–
(26,21,0)	1	0.745	0.9	−7.782	−2.268	0.244	−4.161	0.217	–	–	0.791	0.041	–	–	–	–	<0.0001	–	–	–	–	–
(26,21,0)	2	0.59	0.92	−6.973	−2.341	0.291	−3.958	0.236	–	–	0.827	0.086	0.699	0.074	–	–	<0.0001	–	–	0.14	–	–
(26,10,11)	1	0.534	0.93	−5.391	−2.344	0.195	−4.526	0.158	−4.136	0.169	0.829	0.039	–	–	–	–	<0.0001	0.02	<0.0001	–	–	–
(26,10,11)	3	0.487	0.94	−5.324	−2.345	0.325	−4.651	0.52	−4.074	0.285	0.832	0.143	0.87	0.199	0.791	0.137	0.81	0.27	<0.0001	0.82	0.69	0.78
All (Tree #7)																						
(66,0,0)	1	0.857	0.66	−51.896	−3.118	0.319	–	–	–	–	0.814	0.071	–	–	–	–	–	–	–	–	–	–
(40,26,0)	1	0.477	0.89	−25.418	−2.476	0.147	−4.091	0.173	–	–	0.811	0.041	–	–	–	–	<0.0001	–	–	–	–	–
(40,26,0)	2	0.407	0.9	−25.219	−2.510	0.225	−4.029	0.199	–	–	0.835	0.085	0.773	0.069	–	–	<0.0001	–	–	0.46	–	–
(40,13,13)	1	0.414	0.9	−24.669	−2.510	0.157	−4.281	0.167	−4.067	0.167	0.83	0.042	–	–	–	–	<0.0001	0.21	<0.0001	–	–	–
(40,13,13)	3	0.426	0.9	−23.592	−2.510	0.243	−3.758	0.467	−4.191	0.219	0.833	0.109	0.662	0.163	0.903	0.098	0.006	0.36	<0.0001	0.23	0.15	0.88

*See main text for description of groups.
Pagel's ʎ – parameter representing strength of phylogenetic signal with a maximum of around 1 (strong signal) and minimum of 0 (no signal).
Abbreviations: *n*/grp – number of cases in group, Log(L) – base 10 logarithm of model likelihood, Int. – intercept, S – slope, SE – standard error, XvY – t test comparing difference between indicated parameters, r^2 – coefficient of determination.

recognized three groups, all of the intercepts were significantly different.

Next we assessed whether the PhyANCOVA could be augmented with fossils. Promontorial patency in fossils would be predictable from canal relative size if no promontorially defunct extant taxa plot within the 95% prediction intervals of extant taxa with a patent promontorial artery. We found that the lower prediction confidence interval on the regression of all extant taxa with a consistently patent promontorial artery excludes all extant taxa in which the promontorial artery is sometimes involuted or consistently absent (Fig. 3), suggesting that it is possible to use the area of the promontorial canal to determine the presence or absence of a patent promontorial artery when associated data on endocranial volume are available.

Entering fossil endocranial volumes into regression equation #5 (Table 2), we found that some taxa plotted above the lower prediction confidence interval, while others plotted below (Table 6). Specifically, *Microsyops*, *Leptadapis*, *Notharctus*, *Smilodectes*, *Rooneyia*, *Microchoerus*, *Necrolemur* and all sampled fossil anthropoids plotted above the lower confidence interval for the regression based on extant taxa with a patent promontorial artery, suggesting that they possessed patent promontorial arteries. In contrast, *Ignacius*, *Adapis* and all sampled subfossil lemurs plotted below, suggesting that they lacked patent promontorial arteries.

The results of PhyANCOVA changed slightly when fossils were added (Table 5). Specifically, we re-ran the analysis with the fossil taxa inferred to have patent promontorial arteries added to group #1; *Adapis*, *Archaeolemur*, and *Babakotia* in group #2 (since they have small promontorial canals but have an ossified stapedial canal); and *Ignacius* and *Megaladapis* in group #3 (since they have small promontorial canals and lack ossified stapedial canals).

Instead of supporting the recognition of three groups with distinct intercepts, the more inclusive PhyANCOVA supported a model that combines groups #2 and #3 into a single group and distinguishes it from group #1 in intercept, but not in slope (Tables 4 and 5). Again, patterns of significance in post hoc comparisons of intercepts within models are consistent with this result since all compared slopes were indistinguishable and the intercepts of groups #2 and #3 were never distinguishable from each other, but always distinguishable from group #1 (Table 4).

5.3. Revisiting multiple regression based on ANCOVA results

Since PhyANCOVA showed that promontorial group #1 (in which members have a consistently patent promontorial artery) has a significantly different scaling relationship from the sample combining groups #2 and #3, we reassessed which covariates (BM, ECV or CA) are most strongly correlated with promontorial canal area within each of these subgroups (Table 2: equations #6–14). Multiple regression for the subsample of extant and fossil taxa with a promontorial canal indicative of a consistently patent promontorial artery returned results very similar to the same analysis on the full sample: only endocranial volume explained significant amounts of variance in promontorial canal area when the other two independent variables were held constant (Table 2: equation #10). In contrast, the multiple regression analysis on the other subsample (groups #2 and #3, in which members have a consistently or variably absent promontorial artery) returned a significant positive effect of both endocranial volume and cranial area on promontorial canal area (Table 2: equation #14). Body mass had no significant effect in any analysis when the other two variables were held constant. Variance inflation factors (VIF) for all independent variables in the promontorially patent analysis were below 10 (SOM Table S5). In contrast, the VIF's in the

Table 5
Likelihood Ratio test to determine best ANCOVA model (from Table 2).

Analysis code*	*n* grps	*n* slps	*n* ptrs	log(L)	Best	Worst	LR	df	*p**
Log likelihoods (extant taxa only)					LRT				
1.1.2	1	1	2	−19.68	2.1.3	1.1.1	23.80	1	<0.0001
2.1.3	2	1	3	−7.78	2.2.4	1.1.1	25.42	2	<0.0001
2.2.4	2	2	4	−6.97	2.2.4	2.1.3	1.62	1	0.203
3.1.4	3	1	4	−5.39	3.1.4	2.1.3	4.78	1	0.029
3.3.6	3	3	6	−5.32	3.3.6	2.2.4	3.30	2	0.192
					3.3.6	3.1.4	0.13	2	0.935
Log likelihoods (full sample)					LRT				
1.1.2	1	1	2	−51.90	2.1.3	1.1.1	52.96	1	<0.0001
2.1.3	2	1	3	−25.42	2.2.4	1.1.1	53.35	2	<0.0001
2.2.4	2	2	4	−25.22	2.2.4	2.1.3	0.40	1	0.528
3.1.4	3	1	4	−24.67	3.1.4	2.1.3	1.50	1	0.221
3.3.6	3	3	6	−23.59	3.3.6	2.2.4	3.25	2	0.197
					3.3.6	3.1.4	2.15	2	0.341

*p is computed from a chi square distribution with (LR,df) as the parameters. LR = two times difference between the more complex v. less complex model. Df = the number of parameters by which the more complex model exceeds the less complex model.
*Analysis code gives G.S.P., where G = number of groups, S = number of slopes, and P = total number of parameters estimated.
Abbreviations: *n* grps − number of groups recognized, *n* slps − number of slopes estimated, *n* ptrs − total number of parameters estimated, Log(L) − base 10 logarithm of model likelihood, p = probability.

promontorially involuted analysis reached into the teens for body mass and cranial area, suggesting substantial and potentially problematic multicollinearity; the VIF for endocranial volume remained around 5.

5.4. Correlates of stapedial canal area

Stapedial canal area was found to be significantly correlated with endocranial volume, body mass, cranial area, and promontorial canal area when it was regressed on each of these variables separately (Table 3, equations #15–18). However, promontorial canal area exhibited a much lower probability of no correlation than the other three and explained more variance (Table 3, equation #17). Multiple phylogenetic regression of stapedial canal area including all relevant independent variables at once returned a result in which only promontorial canal area is significantly correlated with stapedial canal area (Table 3, equation #19).

A second analysis included a larger taxonomic sample by excluding endocranial volume (which is not available for *Omomys carteri*, *Shoshonius cooperi*, *Cantius abditus*, or *Carpolestes simpsoni*, for example). Results of bivariate regressions were similar with all three included variables showing a significant correlation with stapedial canal area, and with promontorial canal area having the strongest p-value and explaining the most variance of the three (Table 3, equation #20–22). However, in the multiple regression analysis, stapedial canal area was significantly correlated with only cranial area (Table 3, equation #23).

Table 6
Variables of interest for fossil sample and inferences on promontory reliance.

Taxon	lnECV	lnPA	lnPA prediction	Lower PI*
Megaladapis grandidieri	4.44	−0.215	1.460	0.879(−)
Archaeolemur majori	4.53	−0.920	1.537	0.955(−)
Babakotia radofilai	3.87	−1.031	0.971	0.392(−)
Adapis parisiensis	2.17	−1.808	−0.478	−1.069(−)
Cantius ralstoni	–	−1.783	–	–
Cantius abditus	–	−1.378	–	–
Cantius nuniensis	–	−0.978	–	–
Leptadapis leenhardti	2.31	−0.650	−0.364	−0.954(+)
Notharctus tenebrosus	2.04	−0.991	−0.591	−1.184(+)
Smilodectes gracilis	2.07	−0.499	−0.569	−1.161(+)
Mahgarita stevensi	–	−1.115	–	–
Parapithecus grangeri	2.43	0.506	−0.257	−0.845(+)
Aegyptopithecus zeuxis	2.89	0.863	0.129	−0.454(+)
Antillothrix bernensis	3.70	0.931	0.828	0.248(+)
Dolichocebus gaimanensis	3.10	0.118	0.310	−0.272(+)
Homunculus patagonicus	2.99	0.253	0.217	−0.366(+)
Tremacebus harringtoni	2.79	0.677	0.051	−0.533(+)
Shoshonius cooperi	–	−1.934	–	–
Omomys carteri	–	−2.418	–	–
Microchoerus erinaceus	1.45	−1.616	−1.098	−1.701(+)
Necrolemur antiquus	1.34	−1.483	−1.196	−1.801(+)
Victoriapithecus macinnesi	3.57	0.996	0.716	0.136(+)
Rooneyia viejaensis	1.98	−1.094	−0.646	−1.240(+)
Ignacius graybullianus	0.76	−3.544	−1.686	−2.304(−)
Microsyops annectens	1.77	−1.366	−0.820	−1.417(+)
Afradapis longicristatus	–	−0.924	–	–
Carpolestes simpsoni	–	−3.794	–	–

"ln(PA) prediction" is based on equation resulting from regression of ln(PA) on ECV using a sample including all extant taxa that are promontory reliant ($n = 26$) (equation #5 in Table 2). "Lower PI" is computed from this regression as described in text.
*The symbol in parentheses after the 'Lower PI' value indicates whether the prediction in 'LnPA prediction' is above (+) or below (−) the lower 95% prediction limit.

5.5. Re-assessing the ratio of promontorial canal area to stapedial canal area

We used a number of approaches to evaluate the systematic and functional significance of the ratio of stapedial canal area to promontorial canal area (SA/PA) including phylogenetic t-tests, correlation with promontorial canal area residuals and assessment of intraspecific ranges. Because we were able to infer whether fossil taxa were promontorially reliant through earlier analyses, all fossil species with endocranial volumes could be included in these analyses.

According to phylogenetic t-tests, there is no significant difference in SA/PA values between reliant and non-reliant promontorial groups ($n = 23$, Pagel's $\lambda = 1.0$, $t = -1.12$, $p = 0.27$). Furthermore, the residual of promontorial canal area relative to its estimated relationship with endocranial volume is not significantly correlated with SA/PA values either (Table 3, equation #24).

Finally, both intraspecific ranges and species-specific mean values of SA/PA violate the hypothesis that strepsirrhines can be distinguished from haplorhines by an SA/PA value greater than 1 (Table 1). Intraspecific ranges of *Eulemur*, *Varecia*, *Archaeolemur*, and *Babakotia* show that even though some individuals have a larger stapedial canal, as expected for strepsirrhines, other individuals have a larger promontorial canal (Table 1, Fig. 4). In some instances, this variation is potentially attributable to measurement error. The error study (SOM Table S4) shows that repeated measures of eight individuals result in maximal error of 0.22 (as in

a range of SA/PA = 1.00–1.22) and minimal error of 0.09. This suggests that our result showing that *Eulemur*'s range drops below 1.0 may be an artifact of measurement error since its minimum value for SA/PA is 0.991. Furthermore, *Babakotia radofilai* (DPC 9116) was included in our error study and its observed range was 0.89–1.116. Thus, it is possible that *Babakotia* has a true range that does not exceed 1.0 (a smaller stapedial canal). In contrast, however, *Varecia*'s and *Archaeolemur*'s intraspecific ranges cannot be explained by measurement error as the extreme values deviate from 1.0 by more than 0.22 units in both positive and negative directions. As our intraspecific sample size tends to be quite small, we suspect that more intensive sampling would show additional species to have similarly large ranges.

Furthermore, a number of strepsirrhine taxa exhibit mean values and ranges substantially less than 1.0 (Table 1), contrary to the assumption that strepsirrhines can be recognized by a larger stapedial than promontorial canal. These include *Avahi*, *Indri*, *Lepilemur* and (as discussed above) possibly *Babakotia*. It is unlikely that measurement error could have incorrectly masked a true range in which the ratio is always greater than 1.0 in any of these taxa, because in all cases the minimum SA/PA values fall short of 1.0 by much more than 0.22 units. However, it is possible that measurement error may have masked a true range that includes 1.0 in *Avahi*, *Indri* and *Babakotia*. In contrast, there is virtually no question that *Lepilemur*'s true range excludes and is below 1.0, since it consistently has a much smaller stapedial canal than promontorial canal.

There is only one sampled fossil taxon with a value both beyond the strepsirrhine range and within the tarsier range of extreme stapedial reduction: the adapiform *Mahgarita stevensi* (Table 1, Fig. 4A). The probable haplorhine *Rooneyia viejaensis* and plesiadapiform *Microsyops* have values beyond all sampled strepsirrhines except *Lepilemur*. While these values have ambiguous phylogenetic significance in the absence of character state optimizations, they may be indicative of a non-patent stapedial artery, since both *Lepilemur* and *Tarsius* lack a patent stapedial artery, apparently unlike any other extant taxa with stapedial canals (Szalay and Katz, 1973; MacPhee and Cartmill, 1986).

We also plot stapedial canal area as a residual of a taxon's predicted promontorial canal area from its endocranial volume (Fig. 4B; Table 2, equation #5). This provides a different view of stapedial relative size, the significance of which we explore in the discussion session.

5.6. Modeling character evolution and ancestral state reconstruction

Directional models were favored for the evolution of endocranial volume on both trees, and for stapedial canal area on the parsimony-based core tree (Table 7, SOM Table S6). The evolution of

Table 7
BayestraitsV2 ancestral state reconstructions.

		ECV**			PA			PA reliance		SA			SA relative
Parsimony core tree		(Directional, no scaling)			(Random walk, kappa)			Confidence*		(Directional, delta)			Size
Node:	*n*d #	Mean	L-HPD	U-HPD	Mean	L-HPD	U-HPD	LPI	UPI	Mean	L-HPD	U-HPD	(SA/PA)
Primatomorpha	na	0.163	−0.515	0.849	−2.177	−3.070	−1.270	−2.88	−1.69	−1.852	−6.203	2.491	0.33
Euprimates	1	0.548	−0.193	1.299	−2.218	−3.088	−1.333	−2.53	−1.36	−1.987	−4.663	0.616	0.23
crown Haplorhini	3	0.611	−0.194	1.410	−1.752	−2.669	−0.870	−2.47	−1.31	−2.146	−4.814	0.512	−0.39
crown Anthropoidea	4	2.239	1.742	2.741	0.314	−0.509	1.179	−1.02	0.11	−5.821	−7.096	−4.540	na
crown Platyrrhini + *Homunculus*	5	2.756	2.249	3.257	0.374	−0.436	1.174	−0.56	0.56	−8.493	−9.701	−7.306	na
crown Catarrhini	6	3.447	2.800	4.118	1.267	0.408	2.140	0.05	1.17	−8.773	−10.346	−7.227	na
crown Cercopith + *Victoriapithecus*	7	3.585	3.249	3.926	1.155	0.378	1.930	0.17	1.29	−9.122	−9.886	−8.347	na
crown Hominoidea	8	4.887	4.206	5.575	1.899	1.059	2.723	1.31	2.45	−8.860	−10.374	−7.325	na
Adapiforms + crown Strepsirrhini	9	1.409	0.702	2.111	−1.823	−2.701	−0.940	−1.76	−0.61	−1.700	−3.330	−0.070	0.12
crown Strepsirrhini	10	1.436	0.596	2.262	−1.862	−2.785	−0.949	−1.74	−0.59	−2.211	−4.424	−0.043	−0.35
crown Lemuriformes	11	1.651	0.647	2.640	−1.516	−2.462	−0.637	−1.54	−0.40	−2.027	−4.666	0.613	−0.51
crown Lemuriformes − *Daubentonia*	12	2.108	1.322	2.893	−1.541	−2.451	−0.653	−1.14	0.00	−3.191	−5.014	−1.299	−1.65
crown Cheirogaleidae	13	1.411	0.593	2.241	−2.787	−3.647	−1.888	−1.76	−0.61	−6.284	−8.201	−4.420	−3.50
crown Lorisiformes	14	1.462	0.398	2.448	−2.371	−3.279	−1.447	−1.71	−0.57	−6.873	−9.373	−4.416	−4.50
Bayesian core tree		(Directional, no scaling)			(Random walk, kappa)			Confidence*		(Random walk, delta)			(SA/PA)
Node:	*n*d #	Mean	L-HPD	U-HPD	Mean	L-HPD	U-HPD	LPI	UPI	Mean	L-HPD	U-HPD	
Primatomorpha	na	0.119	−0.588	0.8077	−1.8	−2.8083	−0.8326	−2.92	−1.73	−4.68	−8.4587	−0.841	−2.88
Euprimates	1′	0.525	−0.1872	1.2563	−2.21	−3.1767	−1.2515	−2.55	−1.38	−3.69	−5.7289	−1.6948	−1.48
Omomyiforms+Haplorhini	2′	0.585	−0.1865	1.3759	−1.95	−2.908	−1.0183	−2.50	−1.33	−3.53	−5.4572	−1.597	−1.59
crown Haplorhini	3′	0.67	−0.2052	1.54	−1.12	−2.0852	−0.1283	−2.42	−1.26	−4	−6.0673	−1.8992	−2.88
crown Anthropoidea	4′	2.369	1.7596	2.978	0.317	−0.616	1.2712	−0.91	0.22	−8.84	−10.1099	−7.6143	na
crown Platyrrhini + *Homunculus*	5′	2.783	2.2908	3.2948	0.374	−0.5578	1.2917	−0.54	0.59	−9.17	−10.1212	−8.2286	na
crown Catarrhini	6′	3.462	2.8088	4.1212	1.266	0.2821	2.2334	0.06	1.18	−9.19	−10.441	−7.9262	na
crown Cercopith + *Victoriapithecus*	7′	3.589	3.2579	3.9298	1.157	0.2656	2.0863	0.17	1.30	−9.21	−9.814	−8.5916	na
crown Hominoidea	8′	4.902	4.2254	5.5838	1.899	0.9398	2.8267	1.32	2.46	−9.21	−10.405	−8.0066	na
Adapiforms + crown Strepsirrhini	9′	1.44	0.7799	2.0875	−1.69	−2.6673	−0.7363	−1.73	−0.59	−2.34	−3.5629	−1.099	−0.65
crown Strepsirrhini	10′	1.44	0.6481	2.2182	−1.67	−2.4203	−0.897	−1.73	−0.59	−2.35	−3.5616	−1.0933	−0.68
crown Lemuriformes	11′	1.694	0.74	2.6501	−1.41	−2.4201	−0.4206	−1.51	−0.37	−3.06	−5.1077	−0.9964	−1.65
crown Lemuriformes − *Daubentonia*	12′	2.139	1.3733	2.9325	−1.5	−2.5005	−0.4753	−1.11	0.02	−4.15	−5.5498	−2.7319	−2.65
crown Cheirogaleidae	13′	1.434	0.615	2.2516	−2.78	−3.7749	−1.8027	−1.74	−0.59	−6.97	−8.4251	−5.4865	−4.19
crown Lorisiformes	14′	1.494	0.4868	2.4963	−2.29	−3.3185	−1.3002	−1.68	−0.54	−7.81	−9.692	−5.8601	−5.52

*LPI and UPI are computed relative to a regression including all promontory reliant tip taxa (both extant and extinct), which is equation #5 in Table 1. If a node's ASR for PA is greater than LPI, that node is reconstructed as 'promontorially reliant'.
**Below each variable, the evolutionary model parameters are given.
Abbreviations: Cercopith – Cercopithecoidea, ECV – endocranial volume, *n*d# – clade node number (see SOM Figs. S1–S2), L-HPD lower 95% highest posterior density limit, U-HPD – Upper 95% highest posterior density limit, PA – promontory canal cross sectional area, SA – stapedial canal cross sectional area, LPI – lower 95% prediction interval, UPI, upper 95% prediction interval.

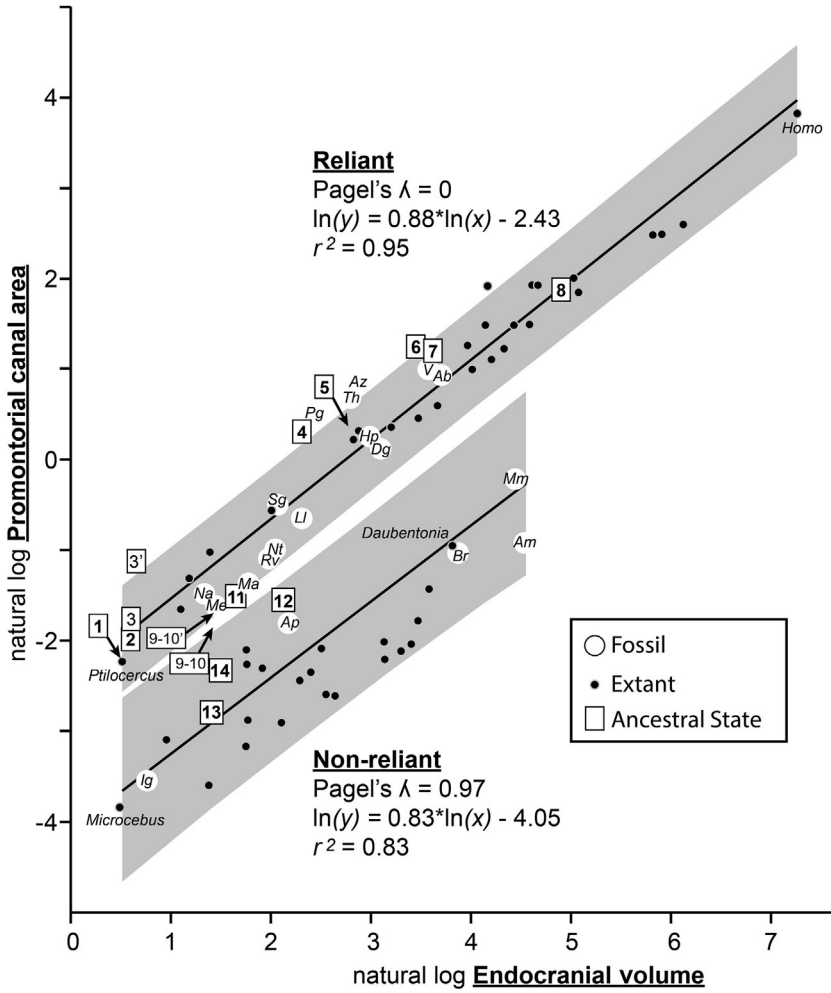

Figure 3. Scaling relationship between promontorial canal cross sectional area (PA) and endocranial volume (ECV). Plot of full dataset of species means for this study. The appropriateness of endocranial volume as the best correlate of promontorial area was determined with multiple regression (Table 2: equation #4). The validity of splitting the data into 'reliant' and 'non-reliant' groups was determined with phylogenetic ANCOVA (Tables 3 and 4). Ancestral state values were determined in BayesTraitsV2. Clade names associated with ancestral node numbers 1–14 are given in Table 6. When ASR nodes numbers are given in bold, mean values from both the Bayesian core tree and parsimony core tree overlap. Otherwise numbers with a 'prime' symbol represent values from the Bayesian tree. Those without are from the parsimony tree. Gray areas represent 95% prediction confidence intervals. Abbreviations for fossil taxa: Ab – *Antillothrix bergensis*; Am – *Archaeolemur majori*, *Ap* – *Adapis parisiensis*, *Az* – *Aegyptopithecus zeuxis*, *Br* – *Babakotia radofilai*, *Dg* – *Dolichocebus gaimanensis*, *Hp* – *Homunculus patagonicus*, *Ig* – *Ignacius graybullianus*, *Lm* – *Leptadapis leenhardti*, *Ma* – *Microsyops annectens*, *Me* – *Microchoerus erinaceus*, *Mm* – *Megaladapis madagascariensis*, *Na* – *Necrolemur antiquus*, *Nt* – *Notharctus tenebrosus*, *Pg* – *Parapithecus grangeri*, *Rv* – *Rooneyia viejaensis*, *Sg* – *Smilodectes gracilis*, *Th* – *Tremacebus harringtoni*.

promontorial canal area was best modeled as a random walk on both trees, as was stapedial canal area on the Bayesian core tree. On the Bayesian tree, all mean ancestral estimates for promontorial canal area were larger than all mean ancestral estimates for stapedial canal area, whereas on the parsimony tree the Primatomorpha, Euprimates, and Adapiformes + crown Strepsirrhini nodes were all characterized by having larger stapedial canal areas than promontorial canal areas.

Computing the residual of reconstructed promontorial canal area relative to reconstructed endocranial volume showed that the following ancestral nodes are above the lower 95% prediction interval for promontorially reliant taxa on both trees: Primatomorpha, Euprimates, omomyiforms+crown haplorhines, and all remaining haplorhine nodes. In addition, the adapiforms+crown strepsirrhines and crown strepsirrhine nodes were reconstructed as promontorial reliant in the Bayesian tree, but below the 95% confidence interval on the parsimony tree. All other strepsirrhine nodes were below the 95% confidence interval for promontorial reliance on both trees (Fig. 3, Table 7).

6. Discussion

6.1. By what criteria can ICA branch size be evaluated?

Over the years, different ways of interpreting the anatomy of the internal carotid (IC) canals have contributed to debate about whether adapiforms share derived anatomical features with haplorhines or strepsirrhines. *Notharctus* and *Smilodectes* have been described as having a relatively small stapedial canal and a large promontorial canal and interpreted as incipiently derived in the haplorhine direction (Gingerich, 1973, 2012; MacPhee and Cartmill, 1986). In contrast, early *Cantius* (Szalay, 1975; Rose et al., 1999) and *Adapis* (Szalay, 1975; MacPhee and Cartmill, 1986) have been described as more closely resembling some extant strepsirrhines in having a relatively small and incompletely ossified promontory canal. Alternatively, some authors have concluded that some adapiforms, such as *Notharctus* (Saban, 1963; Bugge, 1980) and omomyiforms, such as *Omomys* (Ross and Covert, 2000) and *Necrolemur* (Bugge, 1980; Cartmill et al., 1981)

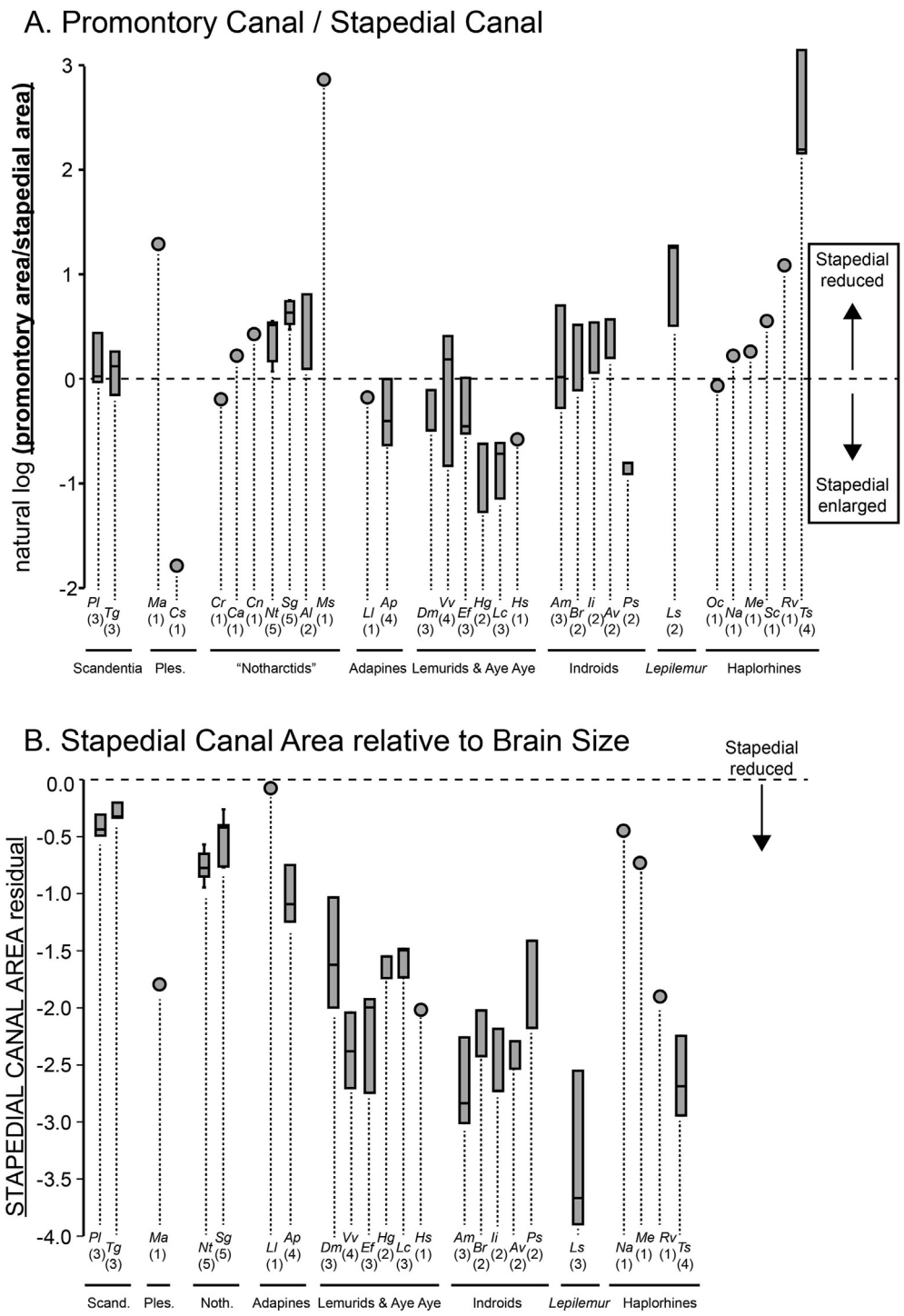

Figure 4. Relative size of stapedial and promontorial canals. **A**, We plot the natural log ratio of promontory canal cross sectional area to stapedial canal cross sectional area so that positive values represent a larger promontorial canal, the value "0" represents canals of equal size, and negative values represent a larger stapedial canal. One problem with this approach is that some taxa have reduced promontorial canals relative to brain size, possibly exaggerating the relative size of the stapedial canal. **B**, We plot relative stapedial canal size in a different way that will not be biased by a species' promontorial canal size as related to promontorial arterial patency: we use residuals from the regression equation predicting promontorial canal area from endocranial volume (In this case the regression equation used for residuals is in Table 2: equation #7; see Fig. 5A for a graphical explanation). Abbreviations not shown in Figure 3: *Pl* – *Ptilocercus lowii*, *Tg* – *Tupaia glis*, *Cs* – *Carpolestes simpsoni*, *Cr* – *Cantius ralstoni*, *Ca* – *Cantius abditus*, *Cn* – *Cantius nuniensis*, *Al* – *Afradapis longicristatus*, *Ms* – *Mahgarita stevensi*, *Dm* – *Daubentonia madagascariensis*, *Vv* – *Varecia variegata*, *Ef* – *Eulemur fulvus*, *Hg* – *Hapalemur griseus*, *Lc* – *Lemur catta*, *Ps* – *Prolemur simus*, *Ii* – *Indri indri*, *Av* – *Avahi laniger*, *Ps* – *Propithecus* sp., *Ls* – *Lepilemur* sp., *Oc* – *Omomys carteri*, *Sc* – *Shoshonius cooperi*, *Ts* – *Tarsius* sp.

exhibit stapedial and promontorial canals that are both "enlarged."

The study that previously went the furthest toward identifying a more objective metric for evaluating IC canal size in primates was conducted by Kay et al. (1992). These authors were the first to quantitatively examine bony correlates of the IC artery (ICA) in the context of an extrinsic variable by examining posterior carotid foramen (PCF) diameter relative to cranial length. This analysis

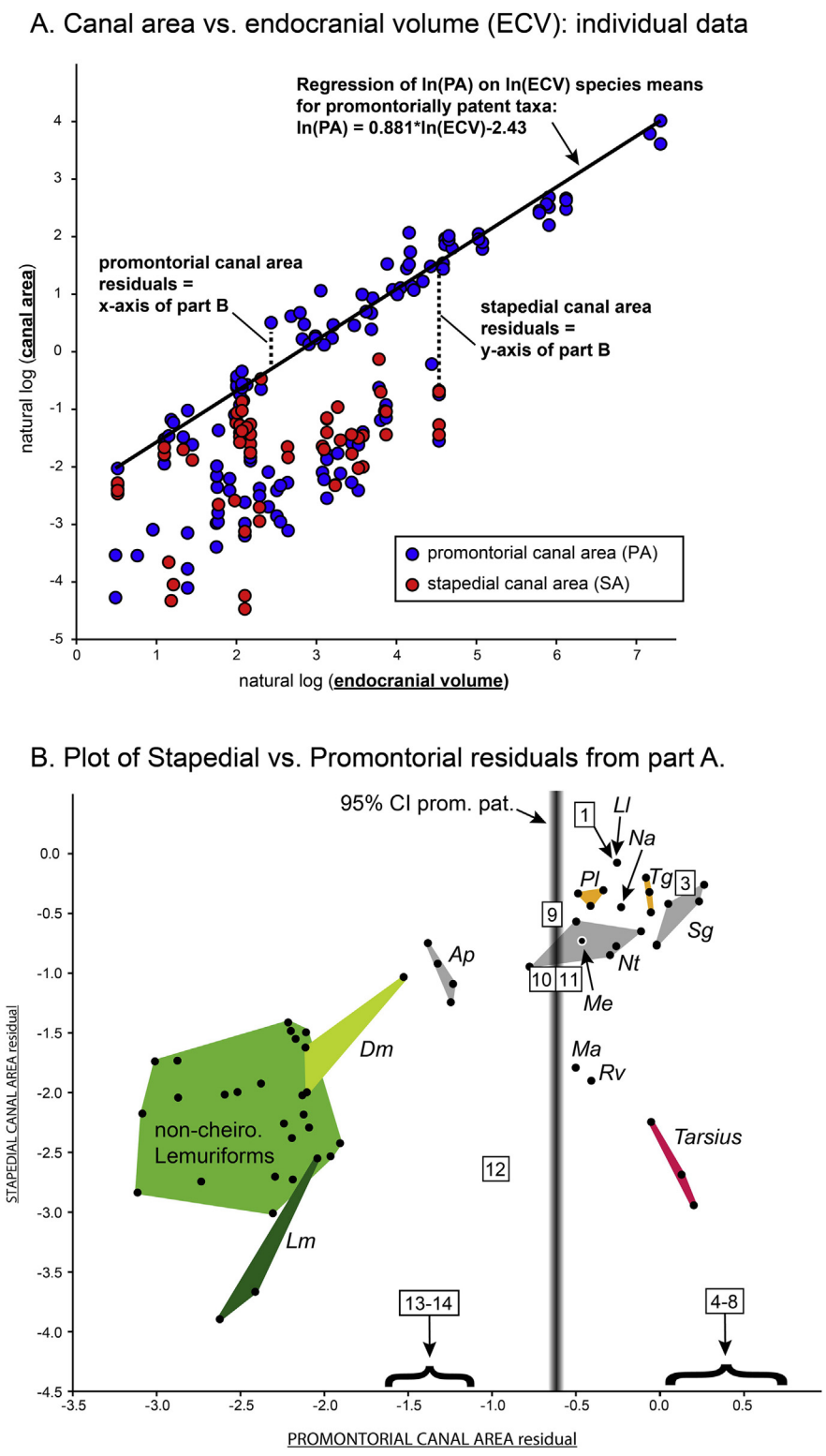

Figure 5. Morphospace of stapedial and promontorial canal area using endocranial volume to control for absolute size A, Against endocranial volumes that represent within species, sex-specific means (data from Isler et al., 2008), we plot both the natural log of promontorial canal cross sectional area (blue dots) and stapedial canal area (red dots) for individuals. We take the regression line relating promontorial canal area to endocranial volume in taxa with a patent promontorial artery (Table 2, equation #7) as the most meaningful line of subtraction for both canal areas. Residuals from this line are plotted in **B**, which is intended to provide a bivariate, size-corrected morphospace for comparing canal dominance patterns. Orange polygons encompass scandentian species, gray polygons encompass adapiform species, olive green encompasses *Daubentonia madagascariensis*, lime-green encompasses non-cheirogaleid lemuriforms including subfossils *Archaeolemur majori* and *Babakotia radofilai*, forest green encompasses *Lepilemur* sp., and red encompasses the tarsiid *Carlito syrichta*. None of the stapedial-lacking taxa is plotted. For simplicity's sake, ancestral state reconstructions are plotted for the parsimony-based tree only. Adding reconstructions from the Bayesian tree would show a significant offset for predicted stapedial residuals (decreased) but not promontorial residuals. Note that omomyiforms and adapiforms plot uniquely with scandentians. *Adapis* is an exception that has become more strepsirrhine-like in reducing its promontorial canal, but not its stapedial canal. This plot suggests the somewhat surprising conclusion that many lemurs – like tarsiers – have a substantially reduced stapedial canal relative to endocranial

demonstrated that the two variables are positively correlated and that the PCF is substantially smaller relative to cranial length in living species that lack a patent ICA. The Kay et al. (1992) study therefore provides a meaningful criterion against which to assess enlargement or reduction of the main stem of the ICA. However, this method does not provide a basis for determining whether the downstream branches of the ICA main stem should be considered "large" or "small" in relative size.

In the present study we have attempted to fill this gap by providing meaningful criteria for evaluating the relative sizes of both the promontorial and stapedial canals. Our multiple regression analysis demonstrates that endocranial volume is the best predictor of promontorial canal cross sectional area among the variables that we analyzed. In fact, body mass and cranial size were not significantly correlated with promontorial canal area after accounting for the effect of endocranial volume in our multiple regression model. When regressed on each variable separately, promontorial canal area had more variance explained by endocranial volume than the others. Further highlighting the utility of endocranial volume as a meaningful variable against which to compare promontorial canal size, our phylogenetic ANCOVA confirmed that taxa with a consistently patent promontorial artery have distinctly larger canals relative to endocranial volume than taxa with an involuted promontorial artery. In fact, the 95% prediction confidence intervals on the "promontorially patent" group do not even overlap the confidence intervals of the "involuted" group.

Researchers have usually assumed that canal enlargement or reduction correlates with arterial patency, importance of the artery in nourishment of its destination structures, and/or the size of the target structures of the traversing artery (Saban, 1963, 1975; Gingerich, 1973; Szalay, 1975; Bugge, 1980; MacPhee and Cartmill, 1986; MacPhee et al., 1988; Gingerich, 2012). Since the primary and only consistent function of the promontorial artery (when patent) is thought to be to supply the brain with blood (Bugge, 1974) our results indicate that future discussions of enlargement or reduction of the promontorial canal may be understood partly as a function of evolutionary changes in absolute brain size.

Multiple regression analyses utilizing subsets of the sample indicate that promontorial canal area may be influenced by more than just brain size in some cases. Multiple regression of the "promontorially patent" group confirms that only endocranial volume significantly correlates with promontorial canal area, as for the analysis of the whole sample. However, in the "promontorially involuted" group, both endocranial volume and head size are significant predictors of promontorial canal area, with each variable explaining about the same amount of variance in promontorial canal area when regressed separately (Table 2, equations #11–12). These results suggest that some interspecific variation in promontorial canal area is the result of factors other than the demands of the brain for blood.

The question of what this different mechanism might be is informed by considering the fact that the promontorial canal has an additional function as the conduit for sympathetic innervation of the head even when the promontorial artery is involuted (MacPhee, 1981; Wible, 1986, 1993; Stern, 1988). If internal carotid nerve size scales with tissue area or volume of distribution, then it makes sense that head size would describe significant amounts of variance in promontorial canal area for species in which the internal carotid nerve is the primary constituent of the promontorial canal. Why endocranial volume still describes so much variation even in taxa with a nonpatent promontorial artery is less clear. It may have to do with the fact that the promontorial artery is an important source of blood for the brain in fetal development even in taxa that develop alternate routes of blood supply to the brain during later ontogeny (MacPhee, 1981; Wible, 1993). Yet another possibility is that the proportions of the nervous system are highly conserved and thus necessarily correlated. Though mechanistically it is unclear why such conservation should exist, the findings of Sherwood et al. (2005) are consistent with this possibility: they show that the best predictor of cranial nerve motor root volumes is medulla volume with little phylogenetic or behavioral effect on most correlations.

While our analyses of promontorial canal area have led to a physiologically, and presumably taxonomically meaningful criterion for assessing relative canal size, the implications of our analyses of stapedial canal area were not as obvious due to the fact that different variables correlated with stapedial canal area in different versions of our multiple regression analyses. One issue that likely reduced the resolution of the results obtained from the stapedial canal area analyses is the smaller sample size of taxa retaining a stapedial canal. In fact, the limited distribution of stapedial canals strictly prohibited the ANCOVA approach for assessing an effect of arterial patency on canal size, since only two taxa (*Tarsius* and *Lepilemur*) bearing a stapedial canal are known to have an occasionally or consistently involuted stapedial artery.

We consider our results as consistent with previous suggestions that the stapedial artery has different roles in treeshrews and non-cheirogaleid lemuriforms (groups in which it is large and patent) in terms of how important it is in supplying blood to the brain meninges, and the other structures of the head (Bugge, 1974; Cartmill and MacPhee, 1980; Wible, 1987). This conclusion is specifically supported by the observation that 1) the stapedial cross sectional area does not correlate with endocranial volume or cranial area in the multiple regression analysis that includes both these variables (Table 3, equation #19), and 2) is more weakly correlated with these variables than promontorial canal area or body mass in bivariate context (Table 3, equations #16, #18). Though stapedial canal area is significantly correlated with promontorial canal area in the first multiple regression analysis (Table 3, equation #19) and cranial area in the second (Table 3, equation #23), we note that in the bivariate context, it is always promontorial canal area that has the strongest statistical correlation and describes the most variance in stapedial canal area (Table 3, equations #16–18, #20–22). We interpret this to mean that the promontorial canal is the most important variable for explaining variance in stapedial canal area. Nonetheless, reporting stapedial enlargement and reduction relative to the promontorial artery (Fig. 4A) is confounded by our finding that promontorial canal size varies with respect to both endocranial volume and patency of the promontorial artery. To get around this problem, we consider both canal areas with respect to the same 'line of subtraction'. The line of subtraction we use is the regression equation relating promontorial canal area to endocranial volume in taxa with a patent promontorial artery (Table 2, equation #7; Fig. 5A). Plotting residuals of the promontorial canal area from this line against residuals of stapedial canal area from the same line gives us a way of looking at canal area with the effects of absolute size removed (Fig. 5B). This plot provides a quantitative criterion justifying claims that adapiforms and omomyiforms are primitive and treeshrew-like in having "both canals enlarged" for the first time.

volume leading to the question of whether this canal is a mainly vestigial structure in most strepsirrhines, as it is in *Tarsius* and *Lepilemur*. The residual value of promontorial canal area associated with lower 95% confidence prediction interval for promontorial patency is shown as a fuzzy line because its exact value depends on the location along the x-axis, ranging from −0.54 to −0.64 (greater in magnitude at the extreme values of the x-axis). All abbreviations have been defined in previous figure captions. ASR node numbers are given in Table 6.

Examining Figure 5B (or Fig. 4B) should also call into question the assumption that the stapedial artery is typically patent and relied upon in individuals of most non-cheirogaleiid lemuriform species. Note that the residual stapedial canal size of *Lepilemur* and *Tarsius* (taxa known to have involuted stapedial arteries) overlaps that of various other non-cheirogaleid lemuriforms (Figs. 4B and 5B). This fact is hidden when looking at PA/SA ratios (Fig. 4A). Previous studies have verified the patency of the stapedial artery in only two species of non-cheirogaleid lemurs, *Lemur catta* and *Varecia variegata* (Saban, 1963; Bugge, 1974; Conroy and Wible, 1978; MacPhee, 1981). These assessments are based on less than 10 individuals. Coleman and Boyer (2011) actually report that the stapedial artery was unilaterally absent in a specimen of *Eulemur* dissected by them. Unlike the promontorial arteries, the stapedials do not broadly anastomose with one another and cannot annex one another's territory.

The results of our ancestral state reconstruction of stapedial canal area allow us to propose a novel explanation for the more limited taxonomic distribution of the stapedial artery. Specifically, stapedial canal area showed directional evolutionary diminishment in models based on the parsimony tree, which means that through time and phylogeny the mean stapedial canal area tends to decrease. We suggest that this finding is causally linked to directional increases in body mass and/or endocranial volume, as supported by results of evolutionary models here (Table 7) and in other publications (Pagel, 2002; Finarelli and Flynn, 2007; Montgomery et al., 2010; Steiper and Seiffert, 2012; Boyer et al., 2013). We hypothesize that evolutionary increases in brain and body size lead to a diminished stapedial size because of a negatively allometric relationship between the stapes size and both body mass and brain volume. Under this scenario, as lineages evolve larger body sizes, the stapes will increasingly impinge on blood flow requirements, which – all else being equal – appear to require that canal cross sectional area scales with positive allometry to body mass (Holt et al., 1981; Schmidt-Nielsen, 1984; Sutera, 1993; Dawson, 2014). While allometric exponents of ossicular elements are not available for broad comparative samples, Braga et al. (2015) show that the area of the oval window (that tightly fits the stapes footplate) scales with an exponent of 0.330 to body mass for catarrhine primates. For their sample of 'non-catarrhine mammals' the exponent is even lower at 0.267 (Braga et al. 2015: their figure 6). These relationships suggest strong negative allometry, as an isometric slope of an area to volume is 0.666. Given the lack of direct data on ossicle scaling we further tested the idea that negative allometry of ossicle size restricts stapedial artery reliance with a dataset from Coleman and Boyer (2011), adding data on endocranial volume from Isler et al. (2008) (SOM Table S7) and using the Bininda-Emmonds et al. (2007) tree (SOM Part II, tree #5). Using the same phylogenetic generalized least squares regression methods and software as in other analyses of this study, we found that the area of the stapes footplate (as a proxy for the potential area of the obturator foramen that passes the stapedial artery) does indeed scale with strong negative allometry to both body mass and endocranial volume: 0.30–0.31, respectively (where isometry would be 0.66) (SOM Part VI). Assuming that footplate area and oval window area are strongly correlated, our results on footplate area can be considered as a confirmation of results for oval window scaling relative to body mass in Braga et al. (2015). Braga et al. (2015) found an exponent from 0.236 to 0.338 depending on sample composition (see SOM Table S5 of Braga et al., 2015).

From the foregoing it appears that larger animals have a proportionally smaller stapes. We propose that this condition severely restricts maintenance of equivalent functionality of the stapedial artery for species of very different body sizes. As a lineage evolves to larger body size, the possible roles of the stapedial artery apparently become more limited because the maximum amount of blood it can supply becomes more reduced proportionally. Thus the artery becomes less relied upon, more diminished, and more likely to be completely involuted in the adult condition of larger species. We believe this process explains the inverse patterns of directional evolution in stapedial artery canal area and endocranial volume in our dataset.

One question remaining is "why should a negative allometric relationship exist between ossicle size and body size?". We presume that this negative allometry exists because of a similar negative allometry between the size of the organs of hearing and body mass (Braga et al., 2015 show an exponent of 0.111 between cochlear length and body mass). In other words, we expect the size of middle ear components to covary with that of inner ear structures to a large degree so that the two systems can work as an integrated whole in audition. In turn, the scaling relationship between the organs of hearing and brain/body size seems to be a consequence of the fact that cochlear volume (Kirk and Gosselin-Ildari, 2009) and length (Coleman and Boyer, 2012) are strong determinants of hearing frequency sensitivity. The absolute interspecific variation in size of the hearing organs may therefore be constrained by demands on the auditory system, unlike brain size or body size. It is worth noting that even if this hypothesis about constraints on the stapedial artery is correct, it seems that additional, unrelated factors (perhaps still related to hearing specialization) must be responsible for the initial loss of the stapedial artery in stem haplorhines, which are thought to have been small-bodied (Gebo, 2004).

6.2. What was the pattern of ICA evolution in early primates?

In order to understand the phylogenetic significance of relative carotid canal size in fossil euprimates, we need to understand the polarity of variation in this feature: is reliance by the brain on blood from the internal carotid system derived or primitive for Euprimates? Most authors have considered the reliant condition to be primitive (Saban, 1963; Bugge, 1974, 1980; MacPhee, 1981; Wible, 1986), but others have taken the opposite perspective. For example Saban (1975, p83) argued that "primate evolution is characterized by the developing dominance of the carotid over the vertebral system in the arterial irrigation of the brain." Gingerich (1973, 2012) considered the promontorial canal in fossil notharctid adapiforms to be enlarged. He interpreted the enlargement as a derived haplorhine feature. Other pieces of evidence suggesting that a reduced ICA is primitive for Euprimates include 1) the frequent reduction in this canal exhibited by plesiadapiform stem-primates (Gingerich, 1976; MacPhee et al., 1983; Kay et al., 1992; Boyer et al., 2012) and 2) the reduction exhibited by cynocephalid dermopterans (Table 1) (Wible, 1993) that some analyses suggest are more closely related to Euprimates than are treeshrews (Beard, 1993; Bloch et al., 2007; Janečka et al., 2007; O'Leary et al., 2013).

We conclude that a well-developed and consistently patent promontorial branch was primitive for Primatomorpha (but see below) and for Euprimates because our ancestral state reconstructions indicate that the ancestral nodes for these clades had relatively large promontorial canals for their endocranial volumes (node #1: Fig. 3, Table 7). This implies that a relatively large promontorial canal is not a derived haplorhine trait.

The ancestral state reconstruction results are more ambiguous regarding the strepsirrhine radiation due to differing results for some nodes on the parsimony-based tree as compared to the Bayesian tree (nodes #9–10: Fig. 3, Table 7). The parsimony-based tree reconstructions suggest that basal strepsirrhines reduced their promontorial canal quite early in their evolution, implying that

some adapiforms re-evolved large promontorial canals. In contrast, the results from analysis of the Bayesian-based tree actually suggest the reverse – that basal strepsirrhines had patent arteries, implying that adapiforms retained the primitive state.

One might question the parsimony-based tree results for basal strepsirrhine nodes since it implies extensive homoplasy (reversal) in sampled adapiforms, as well as lemuriforms. Potentially unlikely homoplasy among lemuriforms is reflected in the promontorially reliant reconstruction of the basal lemuriform node (node #11: Fig. 3, Table 7). However, the alternative reconstruction, in which canal reduction is delayed, also requires substantial homoplasy. The reconstruction with delayed canal reduction would imply that lemuriforms and lorisiforms reduced their canals independently, and that *Daubentonia* and other lemuriforms reduced their promontorial canals independently again.

While the parallel reduction of the promontorial canal in the aye–aye and other lemuriforms is certainly possible, there are reasons to be suspect of this result. The long-branch separating *Daubentonia* from other lemuriforms (SOM Figs S1 and S2) essentially constitutes a lack of data to constrain model estimates of character evolution here. Missing data – as represented by long branches – is probably especially problematic when comparing variables that are estimated using different statistical models as in the case of promontorial canal area (Brownian motion) and endocranial volume (Brownian motion + directional trend) (Table 7). That is, since 1) *Daubentonia* has a very large brain, but a promontorial canal size typical for its brain size among strepsirrhines, and 2) endocranial volume is reconstructed as evolving directionally while promontorial canal area is stochastic, we can expect that extrapolating *Daubentonia*'s trait combinations over a long branch will magnify the canal area relative to endocranial volume in the estimation of the common ancestor of *Daubentonia* and other lemuriforms.

The effect of missing data on ancestral state reconstructions relating these two characters could be tested by including more fossils. Due to a poor fossil record in Madagascar, it seems unlikely that future fossil discoveries will help to break up the long-branch leading to *Daubentonia*, but early African stem-lemuriforms, stem-lorisiforms, and stem-strepsirrhines could help. As djebelemurids are typically reconstructed as being more closely related to crown strepsirrhines than to other adapiforms, data on their petrosals (Benoit et al., 2013) (not currently available) would certainly be helpful for addressing these ambiguities.

Given our argument about long-branch uncertainty, we consider the implications of the Primatomorpha reconstructions to be poorly supported as well: the branch uniting dermopterans to primates is the second longest in the entire tree. The longest branch unites treeshrews to Primatomorpha and our analyses did not converge here so we could not even report results for this node.

Reconstructions of the development of the stapedial canal in the ancestral euprimate are ambiguous given that results based on the Bayesian tree differ substantially from those based on the parsimony tree. We have primarily relied on the signal from the parsimony tree throughout this study because it matches the fossil record better, and represents a less complex model of phylogenetic reconstruction. In addition, it yields more plausible values for ancestral states of the stapedial canal area. In Figure 5B, residuals from Bayesian tree reconstructions are not even plotted because they are offset from the actual data and create a confusing picture. That is, the stapedial residuals are all much lower, so that not even the ancestral euprimate, strepsirrhine or haplorhine plot near treeshrews and actual fossils (Table 6). The substantial difference in reconstructed stapedial size is probably strongly influenced by the different and more basal positions of two key taxa – *Mahgarita* and *Rooneyia* – in the Bayesian tree (SOM Fig. S1): Both taxa have fairly small stapedial canals. In the Bayesian tree, *Rooneyia* is a sister taxon of crown strepsirrhines (it is a stem haplorhine in the parsimony tree). In the Bayesian tree, the next node down the strepsirrhine stem is a clade of adapiforms with *Mahgarita* as the basal member. The basal strepsirrhine node is next (node #9, Table 7), followed by the Euprimate node (#1).

Most other fossil adapiforms and omomyiforms exhibit fairly large stapedial canals relative to their promontory canals (Fig. 5B). These early diverging taxa also have larger promontorial canals relative to brain size. Therefore we take ancestral state reconstructions based on the parsimony tree as the most plausible and conclude that the stapedial canal was primitively large in Euprimates.

Finally, we interpret our data to suggest that the relative enlargement of the stapedial and promontorial canals in primitive euprimates is shared homologously with scandentians as believed by Saban (1963) and Bugge (1974, 1980) among others (MacPhee, 1981; Wible, 1986; MacPhee et al., 1988; Ross, 1994; Ross and Covert, 2000); however, our analyses were not able to provide stable estimates for the Euarchonta node, as mentioned earlier. It would ultimately require more outgroups to test this idea using ancestral state reconstruction analyses.

6.3. What do ICA canal areas tell us about phylogenetic affinities of early adapiforms and omomyiforms

The aspect of the ICA most frequently considered in assessing haplorhine/strepsirrhine affinities is the relative stapedial canal to promontorial canal size (Gingerich, 1973; Szalay, 1975). In this study, we revisited the information content of this variable when considering intraspecific variation and determined that among all sampled adapiforms and omomyiforms, only *M. stevensi* is outside of the strepsirrhine range. Ancestral state reconstructions discussed above indicate that the strepsirrhine condition of having a relatively large stapedial canal is primitive and therefore not phylogenetically informative with respect to relationships within Euprimates. Furthermore, the condition in *Mahgarita* appears to be convergently haplorhine-like, given currently supported phylogenies which nest it deeply within adapiforms (Kirk and Williams, 2011; Marigó et al., 2016; this study).

Even though *Mahgarita* was the only fossil primate in the haplorhine range, the ratio of stapedial canal area to promontorial canal area in *Rooneyia* may reflect an affinity to haplorhines. Our reason for this conclusion is that, while *Rooneyia* is technically in the strepsirrhine range, the value of its ratio excludes it from the ranges of all strepsirrhines except *Lepilemur*. This suggests that *Rooneyia*, like *Lepilemur* (Szalay and Katz, 1973), had a non-patent stapedial artery as an adult. Given other anatomical evidence (albeit weak: see Kirk et al., 2014; Pattinson et al., 2015) placing *Rooneyia* on the haplorhine side of the tree (Szalay and Delson, 1979; Ross, 1994; Ross et al., 1998; Rosenberger, 2006; Seiffert et al., 2010), we think it is possible that *Rooneyia*'s stapedial canal reduction (more extreme than in any other fossil 'prosimian' except *Mahgarita*) is a homologous synapomorphy with tarsiers and/or anthropoids.

Finally, although our analyses suggested that almost all adapiforms and omomyiforms preserving adequate anatomy had a patent promontorial artery as suggested by Gingerich (1973, 2012), this does not provide evidence for haplorhine affinity given the results of our ancestral state reconstructions. In contrast, *Adapis parisiensis* is the only sampled adapiform that can be inferred to have had an involuted promontorial artery. This result could be interpreted as evidence excluding it from a relationship with haplorhines. On the other hand, its close relative *Leptadapis* appears to have retained a patent promontorial canal. Therefore, unless

these two taxa are not as closely related as generally believed (Szalay and Delson, 1979; Seiffert et al., 2015; this study), it seems unlikely that *Adapis*' promontorial reduction is homologous to the reduction exhibited by living strepsirrhines.

While this study does not confirm the contention of Gingerich (1973, 2012) and Saban (1963) that promontorial reliance is derived within primates, more could be done to test their hypothesis through ancestral state reconstruction. In a sense, our ancestral state reconstructions were biased against confirming Gingerich's hypothesis because both phylogenies used for reconstruction of ancestral states reflect a strepsirrhine relationship for adapiforms. We suspect that we would have found support for Gingerich's hypothesis that an enlarged promontorial canal is a homologous synapomorphy of living haplorhines, omomyiforms and adapiforms, if we had instead used a tree that placed both adapiforms and omomyiforms on the haplorhine side of the tree. In other words, we think that utilizing Gingerich's preferred phylogeny would reconstruct the euprimate ancestral node as having an involuted promontorial artery because of the proximity of this node to three groups that tend to have small promontorial canals for brain size: strepsirrhines, plesiadapiform stem-primates, and dermopterans.

However, recent analyses confirm the reliability of the information in morphological character matrices that recover adapiforms as strepsirrhines (Pattinson et al., 2015). Therefore, even though we concede that the results of ancestral state reconstructions could change to support a different set of inferences about the evolution of the ICA under a different phylogenetic hypothesis, the phylogenetic topologies we used are the best supported with respect to the position of adapiforms.

7. Summary and conclusions

While the anatomical and functional implications of our data and analyses are fairly unequivocal, the systematic implications of the data are contingent on phylogenetic tree form and should be further tested by future studies.

This study provided detailed comparative evidence 1) relating promontorial canal area to brain size and 2) showing that this relationship is affected by promontorial artery patency. This allowed us to reject the premise utilised in earlier literature that promontorial artery patency can be inferred from its area in relation to the stapedial canal area. We also found evidence suggesting that the amount of tissue in the head requiring sympathetic nerve innervation may drive promontorial canal size in taxa with an involuted promontorial artery.

On the other hand, stapedial canal area exhibited no strong relationship with brain size, head size, or body size proxies. Instead it only correlates significantly and consistently with promontorial canal area. This provides some justification for looking at stapedial canal area as a proportion of promontorial canal area (as traditionally done). We found that – when considering intraspecific variation – tarsiers differ from strepsirrhines in this ratio, but the majority of fossil adapiforms and omomyiforms overlap with strepsirrhines. Only *M. stevensi* has stapedial reduction outside the strepsirrhine range.

Despite a correlation between the stapedial and promontorial canal area, we were concerned that variation in promontorial canal size due to promontorial arterial involution would confound the meaning of variation in the ratio. Therefore, we suggest that stapedial canal area can be meaningfully reported in the same context as promontorial canal size; that is, as a residual from an equation relating promontorial canal area to endocranial volume (Fig. 5).

Ancestral state reconstructions utilizing phylogenies that place adapiforms in a monophyletic group with extant strepsirrhines suggest that a patent promontorial artery and a large stapedial canal are primitive for euprimates. This, in turn, suggests that fossil taxa cannot be linked to haplorhines on the basis of an enlarged promontorial canal. On the other hand, a reduced promontorial canal has occurred only in strepsirrhine lineages among the euprimates we sampled. Though only strepsirrhines exhibit reduction of the promontorial canal, our results suggest that this reduction happened in multiple lineages independently, and that reduction may not have been a trait of the ancestral crown strepsirrhine. Nonetheless, fossil taxa exhibiting a reduced promontorial canal can be fairly confidently excluded from Haplorhini given character state combinations observed among known taxa. A caveat to our conclusions is that we did not run any analyses using trees that represent adapiforms as haplorhines. Doing so could suggest that an enlarged promontorial canal is derived for haplorhines. However, topologies supporting adapiforms as strepsirrhines currently appear to be extremely robust.

Given patterns of anatomical variation and ancestral state reconstructions, reduced promontorial canal size can be taken as evidence against haplorhine affinities in *Adapis parisiensis*, whereas incipient stapedial canal reduction may reflect a synapomorphy with haplorhines in *Rooneyia*.

Why strepsirrhines tend to involute their promontorial arteries while haplorhines do not and what the effect of promontorial reduction/loss may have been on strepsirrhine brain evolution are intriguing issues brought to light here. We suspect that the loss of the promontory circuit in strepsirrhines diminishes the potential for increasing blood flow and cerebrum size in this group. Conversely, the exceptionally large promontorial canals of early anthropoids (*Parapithecus*, *Aegyptopithecus*, and *Tremacebus*) (and as reflected in basal anthropoid ancestral state reconstructions: Fig. 3, Table 6) may have been a precondition for brain size increases in anthropoid descendant lineages. Future studies may be able to address these questions by adding data on the vertebral arteries. If lower blood flow potential has limited lemuriform encephalization, the vertebral artery cross-sections of these animals should not reach or exceed the combined area of the vertebral arteries and promontory arteries in promontorially reliant taxa relative to brain size.

The stapedial artery on the other hand, given its interspecifically diverse tasks, appears to have been easily replaceable by other arteries over the course of primate evolution. We conclude that abandonment of the stapedial circuit has been often caused by lineage specific body size increases, which lead the stapes obturator foramen to impinge on the stapedial artery due to different body mass-related scaling demands on the vascular system and hearing system.

Acknowledgments

We thank institutional curators and collections staff who provided access to fossils and comparative taxa utilized in this study (see “Introduction: institutional abbreviations), and staff of scanning facilities that digitized those specimens (see “Methods: sample”). We thank Dr. Michael Malinzak for creating and measuring endocasts of *Tremacebus* and *Dolichocebus*, the first endocasts of these taxa available for study. Grants supporting this work include: NSF grants: BCS 1552848 (to DMB), BCS 1440742 & 1558555 (to DMB and GFG), BCS 1440588 (to JIB), BCS 1232534 (to RFK and KLA), BCS 0851272 (to RFK). Leakey Foundation grants: SPS#181951 (to KLA). NSERC Discovery grant (to MTS). University support: Hunter College CUNY (CCG); Duke University (DMB). We acknowledge National Museums of Kenya, F. Spoor and J.-J. Hublin for access to CT images of KNM-MB 29100, the scanning of which was funded by the Max Planck Society. Data collection on extant

specimens from the MCZ (the “Lucas and Copes MCZ sample” on MorphoSource) was supported by NSF DDIG #0925793, and a Wenner-Gren Foundation Dissertation Grant #8102 (both to L. Copes).

Appendix A. Supplementary Online Material

Supplementary online material related to this article can be found at http://dx.doi.org/10.1016/j.jhevol.2016.06.002.

References

Beard, K.C., 1993. Phylogenetic systematics of the Primatomorpha, with special reference to Dermoptera. In: Szalay, F.S., McKenna, M.C., Novacek, M.J. (Eds.), Mammal Phylogeny: Placentals. Springer-Verlag, New York, pp. 129–150.

Benoit, J., Essid el, M., Marzougui, W., Khayati Ammar, H., Lebrun, R., Tabuce, R., Marivaux, L., 2013. New insights into the ear region anatomy and cranial blood supply of advanced stem Strepsirhini: evidence from three primate petrosals from the Eocene of Chambi, Tunisia. J. Hum. Evol. 65, 551–572.

Bininda-Emonds, O.R.P., Cardillo, M., Jones, K.E., MacPhee, R.D.E., Beck, R.M.D., Grenyer, R., Price, S.A., Vos, R.A., Gittleman, J.L., Purvis, A., 2007. The delayed rise of present-day mammals. Nature 446, 507–512.

Bloch, J.I., Silcox, M.T., Boyer, D.M., Sargis, E.J., 2007. New Paleocene skeletons and the relationship of plesiadapiforms to crown-clade primates. Proc. Natl. Acad. Sci. 104, 1159–1164.

Boyer, D.M., Seiffert, E.R., 2013. Patterns of astragalar fibular facet orientation in extant and fossil primates and their evolutionary implications. Am. J. Phys. Anthropol. 151, 420–447.

Boyer, D.M., Scott, C.S., Fox, R.C., 2012. New craniodental material of *Pronothodectes gaoi* Fox (Mammalia, “Plesiadapiformes”) and relationships among members of Plesiadapidae. Am. J. Phys. Anthropol. 147, 511–550.

Boyer, D.M., Seiffert, E.R., Gladman, J.T., Bloch, J.I., 2013. Evolution and allometry of calcaneal elongation in living and extinct primates. PLoS ONE 8, e67792.

Boyer, D.M., Yapuncich, G.S., Butler, J.E., Dunn, R.H., Seiffert, E.R., 2015. Evolution of postural diversity in primates as reflected by the size and shape of the medial tibial facet of the talus. Am. J. Phys. Anthropol. 157, 134–177.

Braga, J., Loubes, J.M., Descouens, D., Dumoncel, J., Thackeray, J.F., Kahn, J.L., de Beer, F., Riberon, A., Hoffman, K., Balaresque, P., Gilissen, E., 2015. Disproportionate cochlear length in genus *Homo* shows a high phylogenetic signal during apes' hearing evolution. PLoS ONE 10, e0127780.

Bugge, J., 1974. The cephalic arterial system in insectivores, primates, rodents, and lagomorphs, with special reference to the systematic classification. Acta Anat. 87, 1–160.

Bugge, J., 1980. Comparative anatomical study of the carotid circulation in New and Old World primates: Implications for their evolutionary history. In: Ciochon, R., Chiarelli, A.B. (Eds.), Evolutionary Biology of the New World Monkeys and Continental Drift. Plenum Press, New York and London, pp. 293–361.

Bush, E.C., Simons, E.L., Dubowitz, D.J., Allman, J.M., 2004. Endocranial volume and optic foramen size in *Parapithecus grangeri*. In: Ross, C.F., Kay, R.F. (Eds.), Anthropoid Origins: New Visions. Kluwer/Plenum, New York, pp. 603–614.

Cartmill, M., 1975. Strepsirhine basicranial structures and the affinities of the Cheirogaleidae. In: Luckett, W.P., Szalay, F.S. (Eds.), Phylogeny of the Primates: A Multidisciplinary Approach. Plenum Press, New York, pp. 313–354.

Cartmill, M., MacPhee, R.D.E., 1980. Tupaiid affinities: the evidence of the carotid arteries and cranial skeleton. In: Luckett, W.P. (Ed.), Comparative Biology and Evolutionary Relationships of Tree Shrews. Plenum Publishing Corporation, New York, pp. 95–132.

Cartmill, M., MacPhee, R.D.E., Simons, E.L., 1981. Anatomy of the temporal bone in early anthropoids, with remarks on the problem of anthropoid origins. Am. J. Phys. Anthrop. 56, 3–21.

Catlett, K.K., Schwartz, G.T., Godfrey, L.R., Jungers, W.L., 2010. “Life history space”: a multivariate analysis of life history variation in extant and extinct Malagasy lemurs. Am. J. Phys. Anthropol. 142, 391–404.

Coleman, M., Boyer, D.M., 2012. Inner ear evolution in primates through the Cenozoic: Implications for the evolution of hearing. Anat. Rec. 295, 615–631.

Coleman, M.N., Boyer, D.M., 2011. Relationships between the expression of the stapedial artery and the size of the obturator foramen in euarchontans: Functional and phylogenetic implications. J. Hum. Evol. 60, 106–116.

Conroy, G.C., Wible, J.R., 1978. Middle ear morphology of *Lemur variegatus*: Some implications for primate paleontology. Folia Primatol. 29, 81–85.

Copes, L.E., Kimbel, W.H., 2016. Cranial vault thickness in primates: *Homo erectus* does not have uniquely thick vault bones. J. Hum. Evol. 90, 120–134.

Copes, L.E., Lucas, L.M., Thostenson, J.O., Hoekstra, H.E., Boyer, D.M., 2016. A collection of non-human primate computed tomography scans housed in MorphoSource, a repository for 3D data. Nature Scientific Data 3, 160001.

Dawson, T.H., 2014. Allometric relations and scaling laws for the cardiovascular system of mammals. Systems 2, 168–185.

Finarelli, J.A., Flynn, J.J., 2007. The evolution of encephalization in caniform carnivorans. Evolution 61, 1758–1772.

Gebo, D.L., 2004. A shrew-sized origin for primates. Yearb. Phys. Anthropol. 47, 40–62.

Gingerich, P.D., 1973. Anatomy of temporal bone in Oligocene anthropoid *Apidium* and origin of Anthropoidea. Folia Primatol. 19, 329–337.

Gingerich, P.D., 1976. Cranial anatomy and evolution of Early Tertiary Plesiadapidae (Mammalia, Primates). Univ. of Mich. Papers Paleontol. 15, 1–141.

Gingerich, P.D., 2012. Primates in the Eocene. Palaeobiodiversity and Palaeoenvironments 92, 649–663.

Godfrey, L.R., Jungers, W.L., 2002. Quaternary fossil lemurs. In: Hartwig, W. (Ed.), The Primate Fossil Record. Cambridge University Press, Cambridge, pp. 97–121.

Gonzales, L.A., Benefit, B.R., McCrossin, M.L., Spoor, F., 2015. Cerebral complexity preceded enlarged brain size and reduced olfactory bulbs in Old World monkeys. Nat. Commun. 6, 7580. http://dx.doi.org/10.1038/ncomms8580.

Hammer, Ø., Harper, D.A.T., Ryan, P.D., 2006. PAST: Paleontological statistics software package for education and data analysis, 1.43 ed. University of Oslo, Oslo.

Harrington A., Silcox, M.T., Yapuncich G.S., Boyer D.M., Bloch J.I., First virtual endocasts of adapiform primates. *J. Hum. Evol.*, in press.

Holt, J.P., Rhode, E.A., Holt, W.W., Kines, H., 1981. Geometric similarity of aorta, venae cavae, and certain of their branches in mammals. Am. J. Physiol. 241, R100–R104.

Isler, K., Kirk, E.C., Miller, J.M., Albrecht, G.A., Gelvin, B.R., Martin, R.D., 2008. Endocranial volumes of primate species: scaling analyses using a comprehensive and reliable data set. J. Hum. Evol. 55, 967–968.

Janečka, J.E., Miller, W., Pringle, T.H., Wiens, F., Zitzmann, A., Helgen, K.M., Springer, M.S., Murphy, W.J., 2007. Molecular and genomic data identify the closest living relative of primates. Science 318, 792–794.

Kay, R.F., Thewissen, J.G.M., Yoder, A.D., 1992. Cranial anatomy of *Ignacius graybullianus* and the affinities of the Plesiadapiformes. Am. J. Phys. Anthropol. 89, 477–498.

Kay, R.F., Perry, J.M., Malinzak, M., Allen, K.L., Kirk, E.C., Plavcan, J.M., Fleage, J.G., 2012. Paleobiology of Santacrucian primates. In: Vizcaino, S.F., Kay, R.F. (Eds.), Early Miocene Paleobiology in Patagonia: High-Latitude Paleocommunities of the Santa Cruz Formation. Cambridge University Press, Cambridge, pp. 306–330.

Kirk, E.C., Gosselin-Ildari, A.D., 2009. Cochlear labyrinth volume and hearing abilities in primates. Anat. Rec. 292, 765–776.

Kirk, E.C., Williams, B.A., 2011. New adapiform primate of Old World affinities from the Devil's Graveyard Formation of Texas. J. Hum. Evol. 61, 156–168.

Kirk, E.C., Daghighi, P., Macrini, T.E., Bhullar, B.-A.S., Rowe, T.B., 2014. Cranial anatomy of the Duchesnean primate *Rooneyia viejaensis*: New insights from high resolution computed tomography. J. Hum. Evol. 72, 84–95.

MacPhee, R.D.E., 1981. Auditory Regions of Primates and Eutherian Insectivores: Morphology, Ontogeny, and Character Analysis. S. Karger, New York.

MacPhee, R.D.E., Cartmill, M., 1986. Basicranial structures and primate systematics. In: Swisher, D.R., Erwin, J. (Eds.), Comparative Primate Biology: Systematics, Evolution, and Anatomy. Alan R. Liss, New York, pp. 219–275.

MacPhee, R.D.E., Cartmill, M., Gingerich, P.D., 1983. New Paleogene primate basicrania and the definition of the order Primates. Nature 301, 509–511.

MacPhee, R.D.E., Novacek, M.J., Storch, G., 1988. Basicranial morphology of Early Tertiary erinaceomorphs and the origin of primates. Am. Mus. Nov. 2921, pp. 1–42.

Marigó, J., Roig, I., Seiffert, E.R., Moyà-Solà, S., Boyer, D.M., 2016. Astragalar and calcaneal morphology of the middle Eocene primate *Anchomomys frontanyensis* (Anchomomyini): implications for early primate evolution. J. Hum. Evol. 91, 122–143.

Martin, R.D., 1990. Primate Origins and Evolution: A Phylogenetic Reconstruction. Princeton University Press, Princeton.

Mason, M.J., 2004. Morphology of the middle ear of golden moles (Mammalia, Chrysochloridae). J. Zool. 260, 391–403.

Meng, J., Hu, Y., Li, C., 2003. The osteology of *Rhombomylus* (Mammalia, Glires): Implications for phylogeny and evolution of Glires. Bull. Am. Mus. Nat. Hist. 275, 1–248.

Montgomery, S.H., Capellini, I., Barton, R.A., Mundy, N.I., 2010. Reconstructing the ups and downs of primate brain evolution: implications for adaptive hypotheses and *Homo floresiensis*. BMC Biol. 8, 9.

Nunn, C.L., 2011. The Comparative Method in Evolutionary Anthropology and Biology. University of Chicago Press, 392 p.

O'Brien, R.M., 2007. A caution regarding rules of thumb for variance inflation factors. Quality & Quantity 41, 673–690.

O'Leary, M.A., Bloch, J.I., Flynn, J.J., Gaudin, T.J., Giallombardo, A., Giannini, N.P., Goldberg, S.L., Kraatz, B.P., Luo, Z.-X., Meng, J., Ni, X., Novacek, M.J., Perini, F.A., Randall, Z.S., Rougier, G.S., Sargis, E.J., Silcox, M.T., Simmons, N.B., Spaulding, M., Velazco, P.M., Weksler, M., Wible, J.R., Cirranello, A.R., 2013. The placental mammal ancestor and the post–K-Pg radiation of placentals. Science 339, 662–667.

Orme, D., Freckleton, R., Thomas, G., Petzoldt, T., Fritz, S., Isaac, N., Pearse, W., 2012. Caper: comparative analyses of phylogenetics and evolution in R. R package version 0.5. http://CRAN.R-project.org/package=caper.

Pagel, M.D., 2002. Modelling the evolution of continuously varying characters on phylogenetic trees. In: MacLeod, N., Forey, P.L. (Eds.), Morphology, Shape and Phylogeny. Taylor and Francis, London, pp. 269–286.

Pagel, M.D., Meade, A., 2013. BayesTraits V2 manual. http://www.evolution.rdg.ac.uk/BayesTraitsV2.0Files/TraitsV2Manual.pdf.

Pattinson, D.J., Thompson, R.S., Piotrowski, A.K., Asher, R.J., 2015. Phylogeny, paleontology, and primates: do incomplete fossils bias the tree of life? Syst. Biol. 64, 169–186.

Pirlot, P., Kamiya, T., 1982. Relative size of brain and brain components in three gliding placentals (Dermoptera: Rodentia). Can. J. Zoolog. 60, 565–572.
Radinsky, L.B., 1979. The fossil record of primate brain evolution. 49th James Arthur Lecture on the Evolution of the Human Brain, American Museum of Natural History, pp. 1–27.
Ragan, M.A., 1992. Phylogenetic inference based on matrix representation of trees. Mol. Phylogenet. Evol. 1, 53–58.
Ramdarshan, A., Orliac, M.J., 2015. Endocranial morphology of *Microchoerus erinaceus* (Euprimates, Tarsiiformes) and early evolution of the Euprimates brain. Am. J. Phys. Anthropol. 159, 5–16.
Rasmussen, D.T., 1990. The phylogenetic position of *Mahgarita stevensi*: Protoanthropoid or lemuroid? Int. J. Primatol. 11, 439–469.
Rose, K.D., MacPhee, R.D.E., Alexander, J.P., 1999. Skulls of early Eocene *Cantius abditus* (Primates: Adapiformes) and its phylogenetic implications, with a reevaluation of "*Hesperolemur*" *actius*. Am. J. Phys. Anthropol. 109, 523–539.
Rosenberger, A.L., 2006. Protoanthropoidea (Primates, Simiiformes): A new primate higher taxon and a solution to the *Rooneyia* problem. J. Mam. Evol. 13, 139–146.
Ross, C.F., 1994. The craniofacial evidence for anthropoid and tarsier relationships. In: Fleagle, J.G., Kay, R.F. (Eds.), Anthropoid Origins. Plenum Press, New York, pp. 469–547.
Ross, C., Williams, B., Kay, R.F., 1998. Phylogenetic analysis of anthropoid relationships. J. Hum. Evol. 35, 221–306.
Ross, C.F., Covert, H.H., 2000. The petrosal of *Omomys carteri* and the evolution of the primate basicranium. J. Hum. Evol. 39, 225–251.
Saban, R., 1963. Contribution a l'etude de l'os temporal des primates. Description chez l'homme et les prosimiens. Anatomie comparee et phylogenie, 29. Memo. Mus. Natl. d'Hist. Nat., Paris, pp. 1–368. Series A.
Saban, R., 1975. Structure of the ear region in living and subfossil lemurs. In: Tattersall, I., Sussman, R.W. (Eds.), Lemur Biology. Plenum Press, New York, pp. 83–109.
Schmidt-Nielsen, K., 1984. Scaling – Why is Animal Size so Important? Cambridge University Press, Cambridge.
Seiffert, E.R., Simons, E.L., Boyer, D.M., Perry, J.M., Ryan, T., Sallam, H.M., 2010. A primate of uncertain affinities from the earliest late Eocene of Egypt. Proc. Natl. Acad. Sci. 107, 9712–9717.
Seiffert, E.R., Boyer, D.M., Costeur, L., 2015. Tarsal morphology of *Caenopithecus*, a large adapiform primate from the middle Eocene of Switzerland. PeerJ 3, e1036.
Sherwood, C.C., Hof, P.R., Holloway, R.L., Semendeferi, K., Gannond, P.J., Frahm, H.D., Zilles, K., 2005. Evolution of the brainstem orofacial motor system in primates: a comparative study of trigeminal, facial, and hypoglossal nuclei. J. Hum. Evol. 48, 45–84.
Silcox, M.T., Bloch, J.I., Boyer, D.M., Godinot, M., Ryan, T.M., Spoor, F., Walker, A., 2009a. The semicircular canal system in early primates. J. Hum. Evol. 56, 315–327.
Silcox, M.T., Dalmyn, C.K., Bloch, J.I., 2009b. Virtual endocast of *Ignacius graybullianus* (Paromomyidae, Primates) and brain evolution in early primates. Proc. Natl. Acad. Sci. 106, 10987–10992.
Silcox, M.T., Benham, A.E., Bloch, J.I., 2010. Endocasts of *Microsyops* (Microsyopidae, Primates) and the evolution of the brain in primitive primates. J. Hum. Evol. 58, 505–521.
Simons, E.L., Seiffert, E.R., Ryan, T.M., Attia, Y., 2007. A remarkable female cranium of the Oligocene anthropoid *Aegyptopithecus zeuxis* (Catarrhini, Propliopithecidae). Proc. Natl. Acad. Sci. 104, 8731–8736.
Steiper, M.E., Seiffert, E.R., 2012. Evidence for a convergent slowdown in primate molecular rates and its implications for the timing of early primate evolution. Proc. Natl. Acad. Sci. 109, 6006–6011.
Stephan, H., Frahm, H., Baron, G., 1981. New and revised data on volumes of brain structures in insectivores and primates. Folia Primatol. 35, 1–29.
Stern Jr., J.T., 1988. Essentials of Gross Anatomy. F. A. Davis, Philadelphia.
Sutera, S.P., 1993. The history of Poiseuille's law. Ann. Rev. Fluid Mech. 25, 1–20.
Szalay, F.S., 1975. Phylogeny of primate higher taxa: the basicranial evidence. In: Luckett, W.P., Szalay, F.S. (Eds.), Phylogeny of the Primates: A Multidisciplinary Approach. Plenum Press, New York, pp. 91–126.
Szalay, F.S., Delson, E., 1979. Evolutionary History of the Primates. Academic Press, San Diego.
Szalay, F.S., Katz, C.C., 1973. Phylogeny of lemurs, galagos and lorises. Folia Primatol. 19, 88–103.
Tacutu, R., Craig, T., Budovsky, A., Wuttke, D., Lehmann, G., Taranukha, D., Costa, J., Fraifeld, V.E., de Magalhães, J.P., 2013. Human ageing genomic resources: integrated databases and tools for the biology and genetics of ageing. Nucleic Acid Res. 41, D1027–D1033.
Visualization Sciences Group, 2009. AVIZO, Version 8.1. Mercury Computer Systems, Burlington.
Wible, J.R., 1986. Transformations in the extracranial course of the internal carotid artery in mammalian phylogeny. J. Vert. Paleontol. 6, 313–325.
Wible, J.R., 1987. The eutherian stapedial artery: character analysis and implications for superordinal relationships. Zool. J. Linn. Soc. 91, 107–135.
Wible, J.R., 1993. Cranial circulation and relationships of the colugo *Cynocephalus* (Dermoptera, Mammalia). Am. Mus. Nov. 3072, 1–27.
Wible, J.R., 2011. On the treeshrew skull (Mammalia, Placentalia, Scandentia). Annals Carnegie Mus. 79, 149–230.
Wible, J.R., Martin, J.R., 1993. Ontogeny of the tympanic floor and roof in archontans. In: MacPhee, R.D.E. (Ed.), Primates and Their Relatives in Phylogenetic Perspective. Plenum Press, New York, pp. 111–148.
Zar, J.H., 1984. Biostatistical Analysis. Prentice-Hall, Englewood Cliffs.